

Effect of halide alteration on Structural and Optical Properties of $\text{CsPbCl}_{3-x}\text{Br}_x$

A dissertation for

PHY 651

Credits: 16

Submitted in partial fulfilment of Masters Degree

M.Sc. in Physics

by

RUSHIKESH V. KHALAP

Roll Number: 22P0430032

ABC ID: 993-286-093-435

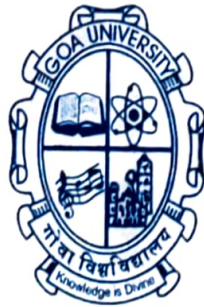
PRN: 201905818

Under the supervision of

Dr. Pranav P. Naik

School of Physical and Applied Science

Physics Discipline



Goa University

May 2024



Examined by:

Seal of the School

DECLARATION BY STUDENT

I hereby declare that the data presented in this Dissertation report entitled, "Effect of halide alteration on Structural and Optical Properties of $\text{CsPbCl}_{3-x}\text{Br}_x$ " is based on the results of investigations carried out by me in the Physics Discipline at the School of Physical and Applied Sciences, Goa University under the Supervision of Dr. Pranav P. Naik. and the same has not been submitted elsewhere for the award of a degree or diploma by me. Further, I understand that Goa University or its authorities will be not be responsible for the correctness of observations / experimental or other findings given the dissertation.

I hereby authorize the University authorities to upload this dissertation on the dissertation repository or anywhere else as the UGC regulations demand and make it available to any one as needed.



Name: Mr. Rushikesh V. Khalaap

Roll no:22PO430032

Date: 08/05/2024

Place: Goa University

COMPLETION CERTIFICATE

This is to certify that the dissertation report “**Effect of halide alteration on Structural and Optical Properties of CsPbCl_{3-x}Br_x**” is a bonafide work carried out by Mr. Rushikesh V. Khalap under my supervision in partial fulfilment of the requirements for the award of the degree of M.Sc. in Physics at the School of Physical and Applied Sciences, Goa University.



Signature and name of Supervising Teacher: Dr. Pranav P. Naik

Date: 08/15/2024



Dean: Prof. Dr. Ramesh. Pai.

Date: 08/05/2024

Place: Goa University



School Stamp

ACKNOWLEDGEMENT

I am pleased to present the report of my project work undertaken during my final year in M.Sc. Physics. Although I have worked hard for the success of this project, it would not have been possible without the help and guidance of some people. Therefore, I would like to express my deep gratitude to those individuals.

Firstly, I would like to thank my project guide, Dr. Pranav P. Naik, for his excellent guidance, encouragement, intelligence and invaluable insight throughout the project. Thank you, Sir, for always motivating and inspiring me. Secondly, I would like to thank Ms. Sugania Chandavelou for her constant help and support throughout the project. Also, I would like to express my heartfelt gratitude towards the faculty members of the Department of Physics (SPAS) at Goa University for their continuous support and for creating a stimulating learning environment. I would like to thank the School of Physics and Applied Sciences for providing me with all the required instruments for my project work.

Next, I want to acknowledge all the PhD students in the Physics department who have assisted me by explaining how to use different instruments and software. I am also grateful to my family and friends for their unwavering support and encouragement throughout my studies.

Table of Contents

Acknowledgement.....	i
Table of Figures.....	iv
Abstract.....	vi
CHAPTER 1: INTRODUCTION	1
1.1 What is Perovskites ?	1
1.2 HALIDE PEROVSKITES	3
1.3 PROPERTIES	3
1.3.1 Structural Properties.....	3
1.3.2 Electronic properties.....	4
1.3.3 Optical properties	6
1.4 APPLICATIONS	8
1.4.1 Perovskite Light-Emitting Diodes (PeLEDs):	8
1.4.2 Photodetectors	9
1.4.3 Solar cells	11
1.5 Effect of halide on properties of perovskites	12
1.6 Aim of the Project	13
References.....	14
CHAPTER 2: LITERATURE REVIEW	16
References.....	23
CHAPTER 3: METHODS OF PREPARATION	25

3.1 Hydrothermal method	25
3.2 Solvothermal method	26
3.3 Hot injection method.....	27
3.4 Mechanochemical synthesis.....	28
3.5 Sol gel method	29
3.6 Ligand assisted reprecipitation method (LARP)	30
References.....	32
CHAPTER 4: CHARACTERISATION TECHNIQUE.....	33
4.1 UV Vis spectroscopy.....	33
4.2 Raman spectroscopy	35
4.3 Scanning electron microscopy	36
4.4 Photoluminescence (PL) spectroscopy	39
4.5 X-ray diffraction (XRD)	40
References.....	42
CHAPTER 5: RESULT AND DISCUSSION	44
5.1 XRD analysis	44
5.2 UV Vis Spectroscopy analysis.....	48
5.3 Photoluminescence spectroscopy analysis.....	53
5.4 Scanning Electron Microscope Analysis.....	56
5.5 Raman spectroscopy analysis	60
References.....	63
CHAPTER 6: CONCLUSION.....	64

Table of Figures

Figure 1: Structure of CaTiO_3	1
Figure 2: Structure of Halide Perovskites [11].	2
Figure 3: Steps for synthesis of samples	31
Figure 4: Schematic diagram of UV-Vis spectroscopy [6].	33
Figure 5: Figure showing stokes, anti-stokes, Rayleigh scattering [7].	35
Figure 6: Schematic diagram of Scanning Electron Microscope [8].	36
Figure 7: Schematic diagram of X-Ray Diffraction [9].	41
Figure 8: XRD spectra of CsPbCl_3	45
Figure 9: XRD of $\text{CsPbCl}_2\text{Br}_1$	45
Figure 10: XRD of $\text{CsPbCl}_{1.5}\text{Br}_{1.5}$	46
Figure 11: XRD of $\text{CsPbCl}_1\text{Br}_2$	46
Figure 12: XRD of CsPbBr_3	47
Figure 13: Absorption and Bandgap of CsPbCl_3	50
Figure 14: Absorption and Bandgap of $\text{CsPbCl}_2\text{Br}_1$	50
Figure 15: Absorption and Bandgap of $\text{CsPbCl}_{1.5}\text{Br}_{1.5}$	51
Figure 16: Absorption and bandgap of $\text{CsPbCl}_1\text{Br}_2$	51
Figure 17: Absorption and bandgap of CsPbBr_3	52
Figure 18: Figure showing absorption of all samples	52
Figure 19: PL spectra of CsPbCl_3 and $\text{CsPbCl}_2\text{Br}_1$	54
Figure 20: PL spectra of $\text{CsPbCl}_{1.5}\text{Br}_{1.5}$ and $\text{CSPbCl}_1\text{Br}_2$	54
Figure 21: PL spectra of CsPbBr_3 and PL spectra of all samples	55
Figure 22: PL spectra of all samples.....	55
Figure 23: SEM images of CsPbCl_3	56

Figure 24: SEM images of CsPbCl ₂ Br ₁	57
Figure 25: SEM images of CsPbCl _{1.5} Br _{1.5}	58
Figure 26: SEM images of CsPbCl ₁ Br ₂	58
Figure 27: SEM images of CsPbBr ₃	59
Figure 28: Raman spectra of CsPbCl ₃ and CsPbCl ₂ Br ₁	60
Figure 29: Raman spectra CsPbCl _{1.5} Br _{1.5} and CsPbCl ₁ Br ₂	61
Figure 30: Raman spectra of CsPbBr ₃	61
Figure 31: Raman spectra of all samples.....	62

ABSTRACT

Compare to silicon solar cells metal halide perovskite cells offer more flexibility, allowing for the creation of lightweight and adaptable solar panels. Metal halide perovskites (MHPs) is one of the most attractive semiconductor materials that have been studied intensively in the past ten years for photovoltaic and other optoelectronic applications by virtue of their excellent properties including high photon absorption, high Carrier mobility, low exciton binding energy, tunable bandgap and simple, cheap solution processable. Metal halide perovskites has direct bandgap. The synthesis of $\text{CsPbCl}_{3-x}\text{Br}_x$ was done by employing the ligand-assisted reprecipitation (LARP) method at room temperature. All $\text{CsPbCl}_{3-x}\text{Br}_x$ crystallized in cubic phase with $\text{Pm}3\text{m}$ space group. The absorption and emission peak shifted to slightly longer wavelengths with increasing bromine content and the bandgap was found to decreased. Scanning electron microscope (SEM) images revealed uniform cubic morphology of the sample. CsPbCl_3 had three raman active modes and CsPbBr_3 had two active modes.

CHAPTER 1: INTRODUCTION

1.1 What is Perovskites ?

Perovskites, CaTiO_3 which is called as calcium titanium oxide which was discovered by Gustav Rose in the Ural Mountains of Russia in 1839 and is named after Russian mineralogist Lev Alexeievitch Perovski. Perovskite name was given to any material, which crystalize into ABO_3 structure .

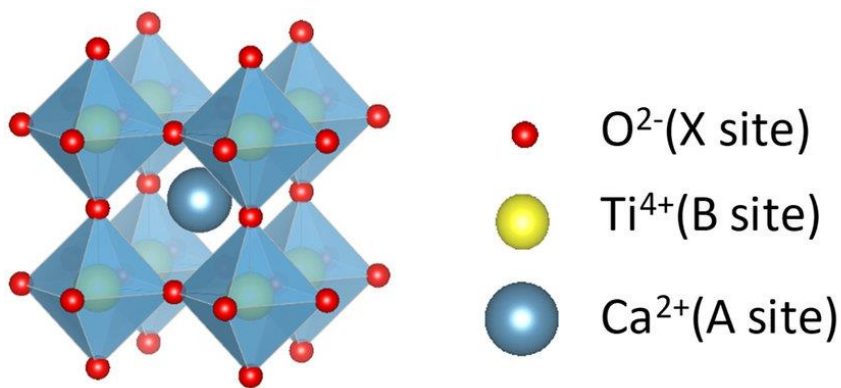


Figure 1: Structure of CaTiO_3

The perovskite formula is denoted by is ABX_3 , in which A cations is heavier that is bigger in size than B atom, and X is halide or oxide which has negative charge (anion) that binds to both cations in perovskite structure. In ideal cubic perovskite structure the B cation is situated at the center having 6-fold coordination forming octahedron of anion (BX_6), X halogen atoms are

situated at the center of each faces in perovskite, and the A cation forms 12-fold octahedral coordination [1].

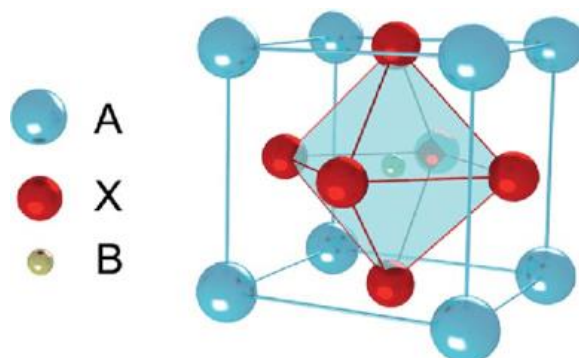


Figure 2: Structure of Halide Perovskites [11].

If A and B sites, both has an inorganic cations group then it will be called as inorganic perovskite. By changing A with organic cations that leads to organic–inorganic hybrid materials [2]. Perovskite materials possess many properties electronic, magnetic, and dielectric properties depend on the crystal structure of perovskite, and to form stable perovskites it should satisfy tolerance factor criteria structure, otherwise it will result in distorted structures. Stability of perovskite materials are mainly determined by Electro neutrality and ionic radii .Goldschmidt tolerance factor estimate the stability of perovskites. One of the interesting thing about perovskite material is that they are simple to prepare and this simple methods sometimes creates interesting chemistry and mechanisms that result in giving rise to unique properties and applications. Hence, it is very important to choosing the correct method for the synthesis is very important since different syntheses methods have their own special features and also important for which compound and applications one is targeting.

1.2 HALIDE PEROVSKITES

Perovskites usually have ABO_3 formula. So in case of halide perovskites the O is replaced by X anion which forming ABX_3 crystal structure. In case Inorganic halide perovskite A site cations consists of inorganic such as Cs^+ , Rb^+ , and B site with metal ion such as Pb or Sn and X with halogen ion such as chlorine bromine and iodine [3]. In case of Organic halide perovskites the A site is occupied by methylammonium and formamidinium [4]. Also we can have double perovskites [5]. So by changing the halide that is chlorine bromine iodine or by changing the A site cation optoelectronic properties may be changed which can be used to target different application such as solar cells ,LEDs etc. By changing the halide or composition the emission can be tuned over the entire visible spectra since the bandgap changes .

1.3 PROPERTIES

1.3.1 Structural Properties

Perovskite is name is given to material which has similar structure and chemical formula has that of calcium titanate ($CaTiO_3$), it was named after named after Russian mineralogist L.A.Perovski. In $CaTiO_3$, the Ti^{4+} metal cation is surrounded by six oxygen atom and the Ca cation situated at the centre of the TiO_6 octahedral network which is formed. In case of metal halide perovskite which has a general formula of ABX_3 and forms stable cubic crystal structure , where A is a monovalent cation, which can be organic such as methylammonium (MA^+),

formamidinium, (FA⁺) or inorganic such as cesium, (Cs⁺), B is a divalent metal cation such as lead, tin and X is a halide or can be mixture of halides of iodide, bromide, chloride [6]. They are bound together by ionic bonding, which allows easy fabrication at room temperature of perovskite. The formation of stable perovskites is done using Goldschmidt tolerance factor (t) which can also determine distortion of the crystal structure. Tolerance factor is defined as ratio of the ionic radius of each of the components in the compound according to equation

$$t = \frac{r_A + r_X}{\sqrt{2}(r_B + r_X)}$$

Where r_A , r_B and r_X are the ionic radius of A, B and X, respectively.

$t = 1$ determines a perfect cubic structure although for metal halide perovskite it ranges from 0.9-1 to maintain a cubic structure with little bit of geometric strains and crystal distortions. Beside this value or range different structure will be formed, such as orthorhombic, tetragonal or hexagonal Structure. According to this rule, only few A site cation including Cs, methylammonium (MA) and formamidinium (FA) can give rise to stable cubic phase MHP.

1.3.2 Electronic properties

The properties of perovskite oxides are mainly dependent on the B-site cations. The size of the A cation can result in the distortion B-X bond. Therefore band structure changes by changing the cation from MA to Cs due to size effect. The electronic states change from 3p to 4p to 5p

by changing the halide from Cl to Br to I. The electrical properties such as charge carrier mobility, diffusion length and carrier lifetime are very important for the application of metal halide perovskites in the field of optoelectronic devices. The carrier mobility determines the ability of charge carrier such as electron and hole to transport within the material. The Diffusion length determines the distance of motion of charge by diffusion and the lifetime determines the time taken by the charges for recombination. These parameters are important for metal halide perovskites to determine the performance of the devices. Metal halide perovskites generally has very long diffusion length, which can be from 1micrometer to more than 170 micrometer which depends on on chemical composition, morphology of metal halide perovskites, and the structure of the device. Halide perovskites are found to have numerous applications due to their exceptional electronic properties [7]. By changing the B-site ion bandgap can also be tuned. Halide Organic inorganic Perovskites semiconductors have direct-bandgap with bandgaps ranging from approximately 1.2 to 2.8 eV. In organic inorganic perovskite, the A-site cation can also change band gap as amine cations may result in distortion of anionic framework by hydrogen bonding and Van der Waals interactions upon. For organic inorganic type of perovskite structure like MAPbI₃, the conduction band minimum is mainly formed by the 6p states of Pb, with a small amount of the 5p states of I hybridized and valence band maximum is formed from the 5p states of I, mixed with a small amount or percentage of the 6 s states of Pb . Since Metal halide perovskites tent to show good carrier transport properties and long carrier lifetimes they are mostly used photovoltaic applications. The long transport length helps for long distance transport of charges in perovskites thin film. This can be attained by the initial Photoexcited carriers recombining away from the excitation spot which results in regeneration of photons

that is reabsorbed and this result in the formation charge carriers at significant distances away from the initial excitation point .For good charge–carrier separation, the exciton binding energy (EB) should be small which defines the lowest energy required to dissociate electron–hole pair (excitons). In organic inorganics halide perovskite, it photo excitations directly generate free electrons and holes, rather than bound excitons. This is due to low exciton binding energy (≤ 25 meV) which result in charge separation at room temperature .

1.3.3 Optical properties

One of the most fascinating features of perovskites are the emission throughout the whole visible range, achieved is achieved by changing the composition. By substituting halide elements such as chloride, bromine iodide the emission can be tuned of perovskites . By substituting chlorides , bromides and iodides or their mixture the emission can be tuned from 400 nm (blue) to 700 nm (red), of all inorganic-perovskite such as CsPbX_3 ($X = \text{Cl, Br, I,}$ or their mixture) which covers the whole visible region. Another way we can to tune the emission is by replacing the lead with different kind metal ions, or organic molecules. The optical properties of halide perovskites are very important for their exceptional performance in Optoelectronic devices such as photovoltaic and LED applications. They show very High absorption coefficients. The absorption Coefficient of MAPbI_3 was found to be $1.5 \times 10^4 \text{cm}^{-1}$ At 550 nm and $0.5 \times 10^4 \text{cm}^{-1}$ At 700 nm, corresponding to the maximum penetration depth of only 0.66 micrometer for 500nm and 2.0 micrometer for 700 nm light. The absorption peaks of the halide perovskites can be

tuned over the whole visible spectrum by compositional engineering. The conduction band minimum is mainly formed by the 6p states of Pb, with a small amount of the 5p states of halide hybridized and valence band maximum is formed from the 5p states of halide mixed with a small amount or percentage of the 6s states of Pb [8]. So changing the metal ions or halides result in change of Valence band maximum and conduction band minimum and also the bandgap. The substitution organic cation may also affect the energy band structure but the effect is less significant compared to B and X ions because the change in A-site organic cation may affect the length and angle of the B-X bonding. The bandgap can change from 1.64 eV to 1.43 eV by replacing methyl ammonium (MA) cation with formamidinium (FA) cation in MAPbI₃ perovskite. Metal Halide Perovskites has low non recombination and defect tolerance which result in good light emitting. The PL peaks of perovskite can tuned from violet to near-infrared regions by changing the composition.

Because of their small size they completely behave differently from bulk solids that they are very useful for certain applications. In bulk materials, the charge carriers can move freely in the material but in nanocrystals the charge carriers are confined in the three spatial directions of the quantum volume, which changes the energetic structure. The optical properties of nanocrystal are mostly size-dependent. The linewidth of the photoluminescence (PL) peak is dependent to the size dispersion of the NCs, therefore a narrow size distribution is very much important to obtain a pure emission colour, which can be used LEDs lamps. In solar cell application, photon are absorbed by the nanocrystals if its energy exceeds the band gap. NCs can produce multiple excitons and for each photon striking them, which will result in increase of efficiency over conventional semiconductors. Also by changing the size of nanoparticle can

results in change of the bandgap, thus changing absorption which result broader light absorption spectra, making them a promising candidate in tandem Photovoltaic cell applications.

1.4 APPLICATIONS

1.4.1 Perovskite Light-Emitting Diodes (PeLEDs):

Light-emitting diodes has recently attracted a great attention due to their low-temperature synthesis process and excellent device Performance. By different perovskite nanocrystals and manufacturing methods red, green and blue PeLEDs can be developed. Song et al. first reported CsPbX₃ nanocrystals LED . The blue LED emits are 455nm, green at 516nm and orange at 586nm have been fabricated. However, the performance of organic metal halide perovskite-based LEDs is low compare to as that of inorganic metal halide Perovskite-based LEDs because of the low charge transport caused by the large number of long amine ligands on the surface of CsPbX₃ Nanocrystals. Therefore, in order to additionally increase the performance of inorganic metal halide perovskite-Based LEDs, one possible method is by making changes in the structure of LED to increase the charge transport and another possible method is to decrease the amount of organic ligands to improve the charge transport performance on the surface of CsPbX₃ Nanocrystals [9].

In order to develop high performance LED, one of the main difficulties is the presence of a charge inoculation barrier between the charge transport layer and the emitter. In order to

increase charge transport, it is important to design a consistent charge transport layer and emitter, which done by introducing an interface layer. Zhang et al. in the LED with ITO / poly TPD /CsPbBr₃/TPBI/LiF/Al structure a perfluorinated ionomer(PFI) intermediate layer is incorporated between the hole transport layer (poly TPD) and the CsPbBr₃ nanocrystalline layer. The PFI interlayer result in the increase of 0.34 eV in the VBM of poly TPD. Unfortunately, the LED still shows unsteady electroluminescence, and also the signal decays to more or less 50% of its original value after 10 minutes. This shows that in order to increase the alignment of the inorganic metal halide perovskite LED, the matching of the band structure and also the immovability of the light-emitting layer should be measured at the same time. In order to solve these two problems, Shi et al. proposed an all-Inorganic light-emitting diode which resulted in high brightness, luminous efficiency and EQE of the LED having 3809 cdm⁻², 2.25 cdA⁻¹ and 2.39%, respectively. Also when the LED was continuously operated at 10.0 V for 10 about hours, it was noticed that it maintain an initial efficiency of nearly 80%, which determine that the working stability has improved significantly.

1.4.2 Photodetectors

Photodetectors were developed using traditional materials such as Ge, Graphene, Si, ZnO and their heterojunctions, these photodetectors generally has issue at high temperature manufacturing process and also an issue with complex device structures. There is a much need to explore low cost, simple device structure and high-performance photodetectors which is

having Low temperature device assembly technology. The photodetector which are based on CsPbX_3 is composed of heavily doped Si or ITO/polyethylene terephthalate (PET) as the substrate, CsPbX_3 active layer and pre-patterned Gold/aluminium/silver electrode. Recent research has shown that the photodetector which are based on CsPbI_3 thin film shows good on and off photocurrent ratio, and the rise and decay times are 24 And 29 ms, respectively. The wavelengths of the photodetectors which are based on CsPbBr_3 and CsPbI_3 are located at 517 and 630 nm, which are steady with the maximum absorption peaks of CsPbBr_3 NC and CsPbI_3 nanosheets, respectively [9].

Even though the photoresponse of Photodetectors under ultraviolet light is very important, study of photodetector with photoresponse under visible light is also important. Recently research has shown that a high-performance Photodetector under visible light which has good orientation and plasma synergy. They found that by using the recrystallization method to prepare CsPbBr_3 nanocrystals at ambient condition , the photocurrent is increased three times compared to dip coating method, and also the optimized device has a high on/off ratio by spin coating method. By introducing Au Nanocrystals into the photodetector, photocurrent is greatly increased because of the influence of local surface plasmon resonance. Some performance parameters of CsPbX_3 based photodetectors are almost similar commercial Si Photodetectors or even better. Therefore by proper interface design, solution-processed CsPbX_3 nanomaterials are likely to become a candidate material for low-cost, high-performance Photodetectors.

1.4.3 Solar cells

The basic principle of any solar cell is that light is absorbed from the sunlight and creates a potential difference between two electrodes. This phenomenon, known as the Photovoltaic effect. A Solar cell device generally consists of a photo-absorber, which absorbs light and excite electrons (e^-), and there are electrodes are used separate the photogenerated charges that is electrons and holes. Without separating of the photogenerated charges to the two different electrodes there will be no photovoltage will appear. This separation of charges can be done by creating an electric field in the material of the solar cell, which will cause the electrons and holes to move in opposite direction. The separation of charges will result in a current flow which will be used to generates electric power when connected to an external circuit [10].

In solar cell the photo absorbing material is loaded in a mesoporous layer of TiO_2 nanoparticles and it is covered by a layer of the organic hole-Transport material (HTM) that is Spiro-OMeTAD., Fluorine-doped tin-oxide (FTO) is used as a transparent conductive oxide as the front contact and for back contact metallic Gold or silver are used. In solar cell Electron transport layer(ETL) is used to collect and transport the electron and Hole transporting layer (HTL) is used to collect and transport the hole. The basic function of the electron transport layer is to: form an electron selective contact with perovskites light absorbing layer, improve the extraction efficiency of photo generated electrons, prevent the hole migrating to the counter electrode, reduce the recombination of electrons and holes. Properties required in selection of material for ETL: High electron carrier mobility, transparent in visible light ,band structure should match with the

perovskites material, preparation of material to feasible condition and low temperature. Hole transport layer (HTL) HTL is used to collect and transport holes from the perovskites light absorbing layer to promote the separation of electron hole pairs in perovskites materials through cooperating with electron transport layer. Properties required in selection of material for HTL: high hole mobility, Wide band gap, simple solvent treatment process, high film formation ability. Preparation method -One step coating: spin coating mixed AX and PbX_2 solution, Two step coating: spin coating AX after coating with PbX_2 .

1.5 Effect of halide on properties of perovskites

By substituting halide from chlorine bromine to iodine their bandgap can be tuned. So changing the halide or halide composition the bandgap decrease as one goes from Chlorine to bromine to Iodine. So changing the metal ions or halides result in change of valence band maximum and conduction band minimum. This help in targeting different application in the field of optical and electrical. The optical properties such as emission and absorption tuned over entire visible range from 400 nm (blue) to 700 nm (red) since the bandgap value changes. The electronic states changes from 3p to 4p to 5p by changing the halide from of Cl to Br to I. Also by changing the halide the crystal structure of perovskites also changes such as the lattice parameter, both length between B and X of halide perovskites. The carrier mobility within the perovskites is also affected by changing the halide. The morphology of perovskites is also affected.

1.6 Aim of the Project

Among Perovskites family halide Perovskites are one of the most studied perovskites in the recent years. This halide perovskites have attracted great attention due to their excellent Optoelectronic properties which are used in various application.

The aim of our project is to synthesize CsPbCl_3 , CsPbCl_2Br , CsPbClBr_2 , $\text{CsPbCl}_{1.5}\text{Br}_{1.5}$, CsPbBr_3 and to study the structural, morphological and Optical properties of this perovskites

References

- [1] Akkerman QA, Manna L. What Defines a Halide Perovskite? *ACS Energy Lett.* 2020 Feb 14;5(2):604-610. doi: 10.1021/acsenergylett.0c00039. Epub 2020 Jan 28. PMID: 33344766; PMCID: PMC7739487.
- [2] Sunny F, Varghese LM, Kalarikkal N, Subila KB. Metal Halide Hybrid Perovskites. In *Recent Advances in Multifunctional Perovskite Materials 2022* Dec 14. IntechOpen.
- [3] Eperon GE, Paternò GM, Sutton RJ, Zampetti A, Haghighirad AA, Cacialli F, Snaith HJ. Inorganic caesium lead iodide perovskite solar cells. *Journal of Materials Chemistry A.* 2015;3(39):19688-95.
- [4] Ezealigo BN, Nwanya AC, Ezugwu S, Offiah S, Obi D, Osuji RU, Bucher R, Maaza M, Ejikeme P, Ezema FI. Method to control the optical properties: Band gap energy of mixed halide Organolead perovskites. *Arabian Journal of Chemistry.* 2020 Jan 1;13(1):988-97.
- [5] Rehman MU, Wang Q, Yu Y. Electronic, magnetic and optical properties of double perovskite compounds: a first principle approach. *Crystals.* 2022 Nov 10;12(11):1597.
- [6] Liao CH, Mahmud MA, Ho-Baillie AW. Recent progress in layered metal halide perovskites for solar cells, photodetectors, and field-effect transistors. *Nanoscale.* 2023;15(9):4219-35.
- [7] Chen K, Schünemann S, Song S, Tüysüz H. Structural effects on optoelectronic properties of halide perovskites. *Chemical Society Reviews.* 2018;47(18):7045-77.

[8] Chouhan L, Ghimire S, Subrahmanyam C, Miyasaka T, Biju V. Synthesis, optoelectronic properties and applications of halide perovskites. *Chemical Society Reviews*. 2020;49(10):2869-85.

[9] Zhang W, Eperon GE, Snaith HJ. Metal halide perovskites for energy applications. *Nature Energy*. 2016 May 9;1(6):1-8.

[10] Zhang W, Eperon GE, Snaith HJ. Metal halide perovskites for energy applications. *Nature Energy*. 2016 May 9;1(6):1-8.

[11] https://www.researchgate.net/figure/1-Crystal-structure-of-CaTiO3-perovskite_fig5_350788381

[12] <https://quantum-solutions.com/blog/what-are-perovskite-materials/>

CHAPTER 2: LITERATURE REVIEW

Tong Cai, Hanjun Yang et al studied the Cd-doped CsPbCl₃ material which was synthesized using hot injection method. The aim of the study was to study the variation of optical properties on Cd-doping in CsPbCl₃ perovskites nanocrystal. It was found that a new secondary emission at 610 nm is induced by an energy transfer process from photoexcited hosts to Cd-dopants. Intensity ratios of the Cd-to-BG PL peaks increase and then decrease with further increase of the Cd-doping concentration. Lattice constant was found to decrease from 5.60 to 5.51 Å as the doping concentration increases from undoped NCs to the NCs with 11.49% Cd-doping. Also as the increasing doping there is a blue shift in the wavelength. Average lifetime PL-BG was decreased from 8.43 to 2.3 ns with doping. Decay lifetime curve showed lifetime value of 1.32-1.35 ns [1].

Mrinmoy Roy, Vikram, Sucheta Banerjee et al studied the variation of halide from Cl, Br, I in MAPbX₃ nanocrystal. The aim of the study was to study PL, Absorption spectrum with variation in different halide in MAPbX₃ nanocrystal. The material was synthesized using hot injection method. It was found that the XRD spectra of MAPbBr₃, MAPbCl₃ nanoparticles indicate a pure cubic phase of space group Pm-3m and the XRD of MAPbI₃ indicates tetragonal phase which belongs to space group I4cm. It was noted that as "x" increases in MAPbBr_{3-x}I_x, the structure slowly changes from cubic to tetragonal phase. It was found out that when halide of perovskite material changes from Cl to Br to I, the valence orbital of halide changes from 3p to 4p to 5p

respectively which causes a decrease in the band Gap of the perovskite. Compositional tuning of the perovskite phase displays absorption and emission spectra over the full visible range (400 nm to 750 nm). It was noticed that absorption maxima for MAPbCl₃, MAPbBr₃ and MAPbI₃ occurs at 405 nm, 520 nm and 750 nm respectively. Also MAPbI₃ has higher formation energy compared to other Perovskites, which indicates relatively less stability compared to other perovskites. This is because the B1₆ octahedral in MAPbI₃ structure is weaker due to a bigger size ionic size and. The lower value of electro-negativity of iodine ions makes the bonds weaker. The thin film which was prepared was kept for 30 days at ambient condition and it was found out that MAPbI₃, PbI₂ peak starts to emerge after seven days suggesting MAPbBr₃ to be more stable compared to MAPbI₃ [2].

Tom C. Jellicoe, Johannes M. Richter et.al studied the variation of halide in CsSnX₃ (X = Cl, Cl_{0.5}Br_{0.5}, Br, Br_{0.5}I_{0.5}, I) perovskite nanocrystals. The aim of the study was to study the photoluminescence and absorption spectra with change in halide composition in CsSnX₃ nanocrystal. The material was prepared using hot injection method. It was found that the XRD spectra shows CsSnCl₃ produce a cubic structure and CsSnBr₃ and CsSnI₃ form orthorhombic structure. Absorbance and PL measurements of the as-synthesized perovskite nanocrystals in solution and under inert atmosphere revealed optical bandgaps extending from the visible to the near-IR region. The bandgaps of tin-containing perovskite nanocrystals are red-shifted compared to lead-based particles, due to the higher electronegativity of the tin ion occupying the 'B' site in the ABX₃ perovskite structure. Compositional changes of the halide component

allowed tuning of the optical bandgap. In addition to compositional tuning, they also tried adjusting the reaction temperature in the CsSnBr₃ nanocrystal synthesis between 125 and 170 °C which allowed the optical bandgap to be tuned from 630 to 680 nm. They noticed if the particles are exposed to the ambient only for 5 min, they observe a small spectral shift of the tin binding energy toward higher values which is consistent with an oxidation process from Sn(II) to Sn(IV). This change in oxidation state is accompanied by a drop in PL efficiency [3].

Cuili Gai , Dawei He et.al studied the variation of halide on CsPbX₃ perovskites nanocrystal. The aim of the study was to determine the optical properties by change in the composition of halide. The material was prepared using hot injection method. It was found out that all CsPbX₃ showed a high-symmetry cubic phase with the space group pm3m due to the high reaction temperature in the preparation process. The optical properties of these CsPbX₃ was studied by stable photoluminescence and it was found out that an increase in the cation size resulted in a reduction in the optical bandgap, which was 2.90 eV for CsPbCl₃, 2.40 eV for CsPbBr₃, and 2.00 eV for CsPbI₃. The difference in optical properties is due to the difference in the ionic radius of halide ions with six-fold coordination, which was 1.81, 1.96, and 2.20 Å for Cl⁻, Br⁻, and I⁻, respectively. They noticed that CsPbCl₃ perovskite exhibited the PL peak at 434 nm with full width at half maximum (FWHM) = 16 nm (blue color emission) and the CsPbBr₃ perovskite showed PL peak at 507 nm and FWHM = 23 nm (green color emission) and the CsPbI₃ perovskite showed PL peak at 625 nm with FWHM = 37 nm (red color emission). Then they studied influence of mixed halogen cation based on CsPbCl_yBr_{3-y} (y = 0, 0.5, 1, 1.5, 2, 2.5, and 3). They

found that the XRD patterns, the diffraction peaks exhibited successive shift, which was linearly dependent on the halide composition and the cubic Structure is still maintained. From the PL spectra, they also found the successively red shift emission peaks. Then they further studied the influence of mixed halogen cation based on $\text{CsPbBr}_y\text{I}_{3-y}$ ($y = 0, 0.5, 1, 1.5, 2, 2.5, \text{ and } 3$) which showed similar result of $\text{CsPbCl}_y\text{Br}_{3-y}$ perovskite nanocrystal [4].

Parthiban Ramasamy, Da-Hye Lim et.al studied CsPbBr_3 NCs to determine the halide exchange reactions, because they have visible green emission at around 508 nm, which can be tuned either in the blue or red side of the visible spectrum by substituting Br^- with Cl^- or I^- ions. CsPbBr_3 NCs with a size of around 8 nm was synthesized. The aim of the of the study is to focus on optoelectronic properties with change in halide composition. The as-synthesized CsPbBr_3 NCs has a cubic structure. It was found out that the (200) reflection at 30.681 gradually shifted to lower angles for Br to I exchange due to the lattice expansion by the substitution of larger I ion for the smaller Br ion. It was also observed that the change in the intensity of the XRD peaks. They noticed that for the iodide-exchanged samples, the intensity of the (200) plane was very high compared with the other planes. The as-synthesized CsPbBr_3 was having absorbance peak at around 485 nm. With an increase in the concentration of LiI, the absorbance peak gradually red shifted and reached 634 nm for 1.28 M LiI. It was noticed that when LiI was replaced with LiCl, the absorbance and luminescence peaks of CsPbBr_3 were blue shifted to lower wavelengths. This is due to the gradual conversion of CsPbBr_3 to CsPbCl_3 . The CsPbCl_3 NCs exhibited strong absorbance and narrow luminescence peaks (FWHM = 15 nm) [5].

Loredana Protesescu, Sergii Yakunin et.al studied the CsPbX_3 perovskites nanocrystal by variation of halide and their mixed halide. The material was prepared using hot injection method. The aim of the project was to study the cesium lead halide perovskites by changing the halide composition and to determine that it is favorable for optoelectronic material. It was found out that the XRD spectra shift towards lower angle when changing halide from Cl to Br to I, this is due to increase in lattice constant from chlorine to bromine to iodine. It was notice that Optical absorption and emission spectra of colloidal CsPbX_3 NCs can be tuned over the entire visible spectral region by adjusting their composition. Photoluminescence spectra showed red shift in wavelength by variation halide from chlorine to bromine to iodine. Bright photoluminescence of all nanocrystal was observed due to high quantum yield of 50-90% and narrow emission line widths of 12–42 nm. Absorption spectra showed increased in the absorption wavelength from chlorine to bromine to iodine. Time-resolved photoluminescence decays of CsPbX_3 NCs indicate Radiative lifetimes in the range of 1–29 ns with faster emission For wider-gap [6].

Valdi Rizki Yandri, Priastuti Wulandari et.al studied the CsPbCl_3 and CsPbBr_3 perovskites nanocrystal. The material was prepared using Ligand assisted reprecipitation method. In this paper the author had studied the Photoluminescence properties of CsPbCl_3 and CsPbBr_3 Nanocrystals synthesized by LARP Method with Various Ligands and Anti-solvents. The XRD spectra of CsPbCl_3 and CsPbBr_3 nanocrystals showed cubic space group $\text{pm}3\text{m}$. They used OA and LA as Ligands and toluene, THF, and chloroform as anti-solvent. It was found out that

Photoluminescence (PL) peaks of CsPbCl_3 are seen at around 435 nm and CsPbBr_3 at around 516 - 527 nm. Also it was observed that in CsPbCl_3 , for OA, PL peaks are not significantly affected by antisolvent. On the other hand, for LA, PL peaks are affected by antisolvent. In CsPbBr_3 , the PL peaks are also affected by LA ligand. It was also noticed that the PL spectral shape of CsPbCl_3 has a much broader width indicating a different origin and mechanism than PL observed in CsPbBr_3 . CsPbCl_3 form 3 dimensional nanocrystal whereas CsPbBr_3 forms 2 dimensional nanocrystal. The OA ligand, which has an amine group, can form a strong interaction with the CsPbBr_3 NC surface leading to the formation of 2D NCs both in toluene and THF [7].

Min Chen, Yatao Zou et.al studied CsPbX_3 perovskite nanocrystals. The material was prepared using solvothermal method. In this paper the author had studied simple and efficient solvothermal to prepare CsPbX_3 nanocrystals with tunable and bright photoluminescent (PL) properties, controllable composition, and morphology. It was noticed that the XRD spectra shows cubic structure for all the perovskites nanocrystal. It was found out that the peaks shift gradually to lower angles when halide composition is changed from chloride to bromide to iodide, which is due to the increased radii of halide ions from chloride to bromide and iodide. The as prepared CsPbX_3 nanocrystals show bright emission, high PLQY Of up to 80%. They noticed that the emission can be tuned to cover the entire visible spectral range (from 410 to 700 nm) by adjusting the composition of anions. The CsPbCl_3 nanocrystals show a sharp absorption peak at 400 nm and the emission peak is 410 nm with a narrow FWHM of 12 nm. CsPb(Cl/Br)_3 nanocrystals exhibit a bright blue emission with a sharp emission peak at 460 nm

and a narrow FWHM of 16 nm and CsPbBr₃ nanocrystals emit strong green light with an emission peak at 520 nm and a FWHM of 23 nm. They also found out that bright orange and red solution can be obtained for CsPb(Br/I)₃ and CsPbI₃ nanocrystals respectively. They also prepared ultrathin CsPbX₃ (X = Cl/Br, Br, and Br/I) Nanowires. Because of the strong quantum confinement effect they noticed both the absorption and emission peaks of such ultrathin nanowires shift to the shorter wavelength range. As a result, the ultrathin nanowires emit light with totally different colors from nanocubes [8].

References

- [1] Cai T, Yang H, Hills-Kimball K, Song JP, Zhu H, Hofman E, Zheng W, Rubenstein BM, Chen O. Synthesis of all-inorganic Cd-doped CsPbCl₃ perovskite nanocrystals with dual-wavelength emission. *The Journal of Physical Chemistry Letters*. 2018 Dec 4;9(24):7079-84.
- [2] Roy M, Vikram, Banerjee S, Mitra A, Alam A, Aslam M. Composition-Controlled Synthesis of Hybrid Perovskite Nanoparticles by Ionic Metathesis: Bandgap Engineering Studies from Experiments and Theoretical Calculations. *Chemistry—A European Journal*. 2019 Jul 25;25(42):9892-901.
- [3] Jellicoe TC, Richter JM, Glass HF, Tabachnyk M, Brady R, Dutton SE, Rao A, Friend RH, Credgington D, Greenham NC, Böhm ML. Synthesis and optical properties of lead-free cesium tin halide perovskite nanocrystals. *Journal of the American Chemical Society*. 2016 Mar 9;138(9):2941-4.
- [4] Gai C, He D, Wang Y, Wang J, Li J. Engineering of Halide Cation in All-Inorganic Perovskite with Full-Color Luminescence. *Coatings*. 2021 Mar 13;11(3):330.
- [5] Ramasamy P, Lim DH, Kim B, Lee SH, Lee MS, Lee JS. All-inorganic cesium lead halide perovskite nanocrystals for photodetector applications. *Chemical communications*. 2016;52(10):2067-70.
- [6] Protesescu L, Yakunin S, Bodnarchuk MI, Krieg F, Caputo R, Hendon CH, Yang RX, Walsh A, Kovalenko MV. Nanocrystals of cesium lead halide perovskites (CsPbX₃, X= Cl, Br, and I): novel

optoelectronic materials showing bright emission with wide color gamut. *Nano letters*. 2015 Jun 10;15(6):3692-6.

[7] Yandri VR, Wulandari P, Hidayat R. Photoluminescence Properties of CsPbCl₃ and CsPbBr₃ Nanocrystals synthesized by LARP Method with Various Ligands and Anti-solvents. In *Journal of Physics: Conference Series* 2022 Jun 1 (Vol. 2243, No. 1, p. 012120). IOP Publishing.

[8] Chen M, Zou Y, Wu L, Pan Q, Yang D, Hu H, Tan Y, Zhong Q, Xu Y, Liu H, Sun B. Solvothermal synthesis of high-quality all-inorganic cesium lead halide perovskite nanocrystals: from nanocube to ultrathin nanowire. *Advanced Functional Materials*. 2017 Jun;27(23):1701121.

CHAPTER 3: METHODS OF PREPARATION

3.1 Hydrothermal method

Hydrothermal synthesis is a method that is used to synthesis materials by using high-pressure and high-temperature aqueous solutions. In this method water acts as both the solvent and the reaction medium, which result in the formation of various compounds when heated close vessel called Autoclave. An autoclave is usually constructed from thick stainless steel to withstood the high pressure and is fitted with a safety wall. It may be lined with Teflon (Non reactive Material). When autoclave is heated the pressure increases and the water remains liquid above its normal boiling temperature of 373 K which is called superheated water. These conditions when pressure is raised above atmospheric pressure and temperature above the boiling temperature are known as "Hydrothermal method". All the reagents used in this process are lead carbonate, cesium carbonate, hydrogen chloride, hydrogen Bromide and hydrogen iodide and they are used without further purification. CsPbCl₃ perovskites nanocrystal can be synthesized using hydrothermal method by using desired amount of stoichiometry of PbCO₃ and Cs₂CO₃ dissolved in 15 mL of 6 M haloid acid solution such as HCl, HBr, or HI. under constant stirring for approximately 10 min. The mixture reaction is then transferred into a Teflon autoclave that was properly sealed and placed inside a muffle furnace. The temperature of the in hydrothermal method was maintained at 140 °C for 2h. Advantages of hydrothermal method are simple, easy, low cost & environment friendly method [1].

3.2 Solvothermal method

Solvothermal synthesis is a technique similar to hydrothermal synthesis, but it uses organic solvents instead of water as the reaction medium. In this method organic solvents provide a different chemical environment compared to water, leading to the formation of distinct materials and structures. Solvothermal reactions occur at elevated temperatures and pressures, resulting in the formation of specific materials. The solubility of reactants and products in the organic solvent changes with temperature, affecting the composition and morphology of the synthesized materials. Chemicals used in this method are CsOAc, PbX_2 , 1-ODE, OA, OAm, Cs_2CO_3 , trioctylphosphine oxide, hexane, Chloroform, and PMMA Trioctylphosphine. So to start with Oleylamine and oleic acid was degassed for 1 h under vacuum at 100 °C and kept in glovebox before use. In these process cesium acetate or cesium carbonate, PbX_2 (X = Cl, Br, I, or mixed Cl/Br, Br/I), ODE , OA , OAm were loaded into a Teflon-lined autoclave in glovebox, and then reacted at 160 °C in a rolling oven for 30 min. For $CsPbCl_3$, TOP and TOPO are needed to help dissolve $PbCl_2$ in ODE. For $CsPb(Cl/Br)_3$, TOPO was used to dissolve $PbCl_2$ and the reaction system was kept for longer reaction time for about 1 h. For $CsPbI_3$, the mixture was first stirred vigorously at 40 °C for a while to dissolve the precursors, and then maintained at 160 °C for 20 min. In addition, TOP and TOPO are also required to solubilize the PbI_2 . The solution was naturally cooled down to room temperature and the final products were collected by centrifugation. Hexane was added into the crude solution and then the mixture was centrifuged at 8000 rpm for 5 min to remove the residual reactants [2].

3.3 Hot injection method

The hot injection (HI) method is based on injection of a precursor into a hot solution of the precursors containing ligands. The key parameters that enables to control the size, size-distribution, and shape of colloidal NCs synthesized by the HI method are ,the ratio of the surfactants to the precursors, the injection temperature of the cation or anion precursor, the reaction time and the concentration of the precursors. The chemical which are used in this method are Oleic acid, oleylamine, octadecene, Cs_2CO_3 , lead iodide, cesium bromide, cesium chloride, and cesium iodide. Firstly for the preparation of the Cs-oleate: Cs_2CO_3 , ODE, and OA were loaded into a 50 mL three-Necked flask and dried for 30min at 100 °C with stirring and then heated under N_2 to 150 °C until all Cs_2CO_3 reacted with OA (transparent solution). Because Cs-oleate precipitated out Of ODE at below 100 °C, it had to be annealed to 150 °C before CsPbX_3 perovskite synthesis. After this, for the synthesis of CsPbX_3 the PbX_2 ($X = \text{Cl}, \text{Br}, \text{and I}$), OAm , oleylamine , and octadecene were added to a three-necked round-bottom flask (25 mL). Then the mixture was heated to 100 °C with stirring and maintained for 30 min. The mixture was heated to 160 °C until the PbX_2 precursor was completely dissolved. Then, the hot cesium oleate precursor solution was then quickly injected in above mixture. After this the flask was quickly transferred to the ice bath, and the obtained CsPbX_3 was kept by centrifugation at 10,000 rpm for 10 min and stored in cyclohexane before further use. For mixed halide of CsPbX_3 PbX_2 ($X = \text{Cl}, \text{Br}, \text{or I}$) and another PbX_2 ($X = \text{Cl}, \text{Br}, \text{or I}$), OA , OAm and ODE were added to a three-necked round-bottom flask (50 mL). Then, it was heated to 100 °C and stirred for 30 min. Then, it was heated to 160 °C until the PbX_2 precursor was completely dissolved. The hot cesium

OA solution was quickly injected into the above solution, and after this, the flask was quickly transferred to the ice bath. The obtained CsPbX₃ perovskite was kept by centrifugation at 10,000 rpm for 5 min and stored in cyclohexane prior to further use [3].

3.4 Mechanochemical synthesis

Mechanochemical method which results in less waste, solvent-free methods and are used for the synthesis of halide perovskites nanocrystals. The Mechanochemical synthesis method is a process of grinding a material into a very fine powder using a cylinder filled with precursor to be processed and milling ball. The top down approach is used in this method where the bulk particles are crushed to nanoparticles. Kinetic energy that is ball is transferred to sample material placed in the container along with the balls which helps in reducing the size. The milling ball are usually made up of stainless steel, hardened steel, tungsten, carbide. High density and larger size gives better result because they increases the impact energy of collision. Larger ball produces smaller grains size. Filling of milling container should be such that about 50 percent of space is left empty. Because it is necessary that there is enough space for the balls and material to move around freely in container. Less than half filled the efficiency is reduced. Milling speed, at high speed the balls get attached to the walls of container and do not impose any impact force on the material. In this method a mixture of AX and BX₂ such as CsI, and PbI₂ and PbBr₂ precursor powders are placed in a ball mill. During the reaction, energy transfer from the balls to the precursor powders occurs, crushing the reactant materials and result in forming the perovskite which is indicated by color change. For the size and crystallinity of the prepared

perovskite, the bowl rotation speed, the number of milling balls, and the reaction energy are critical parameters. Since these parameters are responsible for the total energy input provided to the system, care must be taken about the heat that is generated internally and, thus, the reaction temperature. If we don't monitor the internal temperature this may affect its specific outcome [4].

3.5 Sol gel method

The Sol-gel method is generally used to synthesize nanomaterials. The principle of Sol-gel method is based on between metal cations and a chelating agent (such as citric acid, or ethylene glycol also ethylenediaminetetraacetic acid (EDTA), oxalic acid, tartaric acid or glucose). Metal ions and chelating agent should be 1:1 in molar ratio. In this method metal alkoxides are used as starting material, which is derivative of the alcohol ROH, where R is an alkyl group or a derivative of metal Hydroxide $M(OH)_x$. Then metal alkoxides dissolved were in alcohol or distilled water at a temperature of 60–80°C under with stirring. In order to avoid the formation of the precipitation pH value of the metal alkoxides solutions must be control and the homogeneous gel will be formed using basic or acidic solutions. It is called hydrolysis and condensation, which brought out formation of polymer chain. The polymer chain improve the viscosity of reaction mixture and produces gel. Then produced gel were beaten and grinded, and then calcined for 5-6 hours at 5500 C to get the pure materials [5].

3.6 Ligand assisted reprecipitation method (LARP)

Cesium lead chloride (CsPbCl_3) and cesium lead bromide and their halide mixture were prepared using LARP Method. The Ligand assisted reprecipitation method was used where Oleic acid were used as ligands. CsCl and PbCl_2 were dissolved in Dimethyl Sulfoxide (DMSO) solvent to form a precursor solution. In this method we measured the raw material to be used using weighing machine. The raw material which was weighed was calculated using stoichiometric calculation. After weighing the precursor were transferred into the beaker which was filled with 15 mL of Dimethyl Sulfoxide (DMSO) which acts as a polar solvent. Then this solution was kept on magnetic stirrer for about 25-30 min till all the precursor was thoroughly mixed. After this around 1.5 mL of oleic acid, which acts as a ligand was added and kept for about 15 min for stirring. Simultaneously toluene was kept in magnetic stirrer in ice bath till the temperature reaches 10-12 degree Celsius. Toluene was used as an antisolvent. Once the toluene was added into the mixture its immediately forms colloidal solution which was kept for about 5 min for stirring. Then the solution was transferred into the centrifuging tube and kept for centrifuging for about 15-20 min. The compound which was formed settled at the bottom. The solution was removed and fresh toluene was added and again kept was centrifuging for 5 min. Then the formed compound was transferred into the petri dish. Then the sample was kept for drying in the furnace at around 90-95 degree Celsius for about 1 hour or more depending on the sample is dried or not. Then the sample was weighed and was characterized [6].

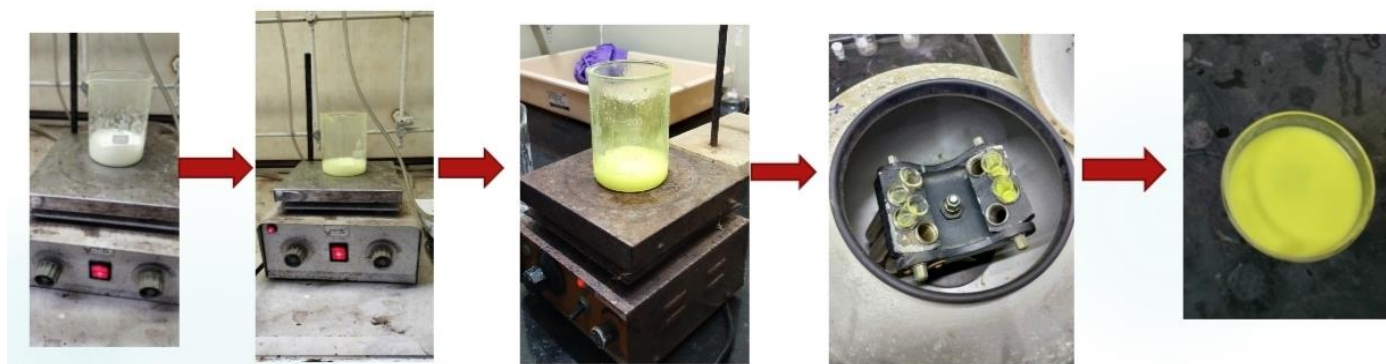


Figure 3: Steps for synthesis of samples

References

- [1] Echeverría-Arrondo C, Alvarez AO, Masi S, Fabregat-Santiago F, Porta FA. Electronic, Structural, Optical, and Electrical Properties of CsPbX₃ Powders (X= Cl, Br, and I) Prepared Using a Surfactant-Free Hydrothermal Approach. *Nanomanufacturing*. 2023 May 19;3(2):217-27.
- [2] Chen M, Zou Y, Wu L, Pan Q, Yang D, Hu H, Tan Y, Zhong Q, Xu Y, Liu H, Sun B. Solvothermal synthesis of high-quality all-inorganic cesium lead halide perovskite nanocrystals: from nanocube to ultrathin nanowire. *Advanced Functional Materials*. 2017 Jun;27(23):1701121.
- [3] Gai C, He D, Wang Y, Wang J, Li J. Engineering of Halide Cation in All-Inorganic Perovskite with Full-Color Luminescence. *Coatings*. 2021 Mar 13;11(3):330.
- [4] Rosales BA, Wei L, Vela J. Synthesis and mixing of complex halide perovskites by solvent-free solid-state methods. *Journal of solid state chemistry*. 2019 Mar 1;271:206-15.
- [5] Review on: Synthesis of perovskite using sol-gel approach. Volume 10, issue 10 February 2022. *International Journal of Creative Research Thought*.
- [6] Yandri VR, Wulandari P, Hidayat R. Photoluminescence Properties of CsPbCl₃ and CsPbBr₃ Nanocrystals synthesized by LARP Method with Various Ligands and Anti-solvents. In *Journal of Physics: Conference Series* 2022 Jun 1 (Vol. 2243, No. 1, p. 012120). IOP Publishing.

CHAPTER 4: CHARACTERISATION TECHNIQUE

4.1 UV Vis spectroscopy

UV-Vis spectroscopy is a technique which is generally used to measure the amount of UV or visible light that is absorbed by or transmitted through a sample with reference to a blank sample. This technique is used to find the bandgap of the material [1]. This technique depends on the use of light. Energy of light which is inversely proportional to its wavelength, therefore shorter wavelengths of light have more energy. Electrons are excited to a higher energy state by absorbing certain amounts of wavelength. Electrons in different shells require a different energy to excite the electrons to a higher energy state. This is why the absorption wavelength changes for different substances. A single xenon lamp can be used for both UV and visible ranges. A tungsten or halogen lamp can be used for visible light and a deuterium lamp is used as a UV light source [2].

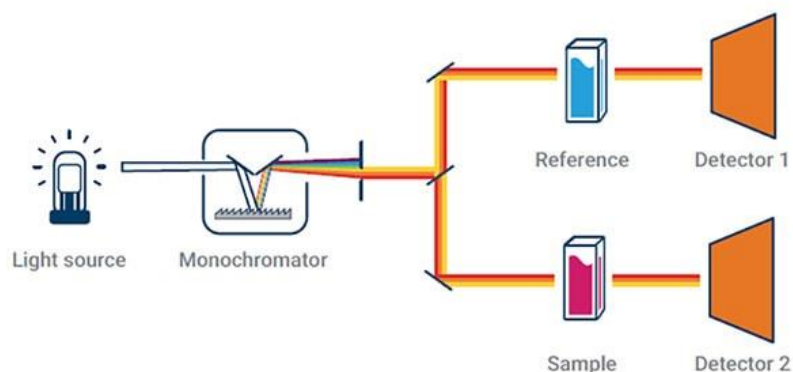


Figure 4: Schematic diagram of UV-Vis spectroscopy [6].

Monochromators – allows only the chosen wavelength of light and absorbs all other wavelength

Monochromators are mostly composed of prisms and slits. The various wavelengths of the light that are separated by prism is then passed to slits. The slit selects a monochromatic beam of light. Beam splitters – splits the beam of light into two halves of equal intensities. One of the two divided beams is then passed through the sample solution and the other beam is then passed through the reference solution. Pair of cuvettes is used in which one is filled with test sample and other one with reference solution. Cuvettes are made of either silica or quartz. Glass can't be used for the cells because it absorbs light in the UV region. After the light has passed through the sample, a detector is used to detect the intensities of the transmitted light coming out of the cuvettes and generate current proportional to the difference in the intensities of sample and blank.

The absorbance (A) is equal to the logarithm of a fraction of the intensity of light passing through reference sample (I_0) divided by the intensity of light passing through the sample (I). If the sample does not absorb light at a particular wavelength then $I=I_0$ and $A=0$. If the sample absorbs light at a particular wavelength then $I<I_0$ and $A>0$. Recording a baseline spectrum using a "blank" reference solution is must. If the instrument is absolutely perfect then the baseline would have zero absorbance for every wavelength.

4.2 Raman spectroscopy

Raman spectroscopy is a technique where scattered light is used to measure the vibrational energy modes of a sample. It is named after C. V. Raman who, together with his research partner K. S. Krishnan, observed Raman scattering in 1928. Raman spectroscopy is based on inelastic scattering of monochromatic light. The Raman effect consists of elastic (Rayleigh) scattering which has the same wavelength as that of the incident light (no energy or momentum is lost between the incident and scattered radiation) and also inelastic (Raman) scattering at different wavelengths because of molecular vibrations. Raman spectra are obtained by exciting the sample with a high-intensity laser beam and passing this scattered light to a spectrometer. The Raman shift is the difference between the energy of the incident and dispersed light. The y-axis of the spectrum represents the intensity of the scattered light, and the x-axis is the wavenumber of the Raman shift (cm^{-1}) [3].

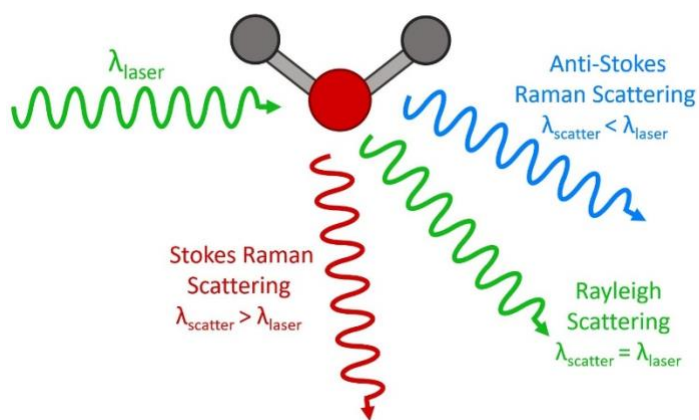


Figure 5: Figure showing Stokes, anti-Stokes, Rayleigh scattering [7].

The Raman shift has two distinct energy bands. Stokes scattering is defined as the shift at wavelengths greater than of the incident light ($h\nu - \Delta E$). Anti-Stokes scattering is defined as the shift at wavelengths shorter than those of the incident light ($h\nu + \Delta E$).

A laser is used as a light source of excitation in Raman spectroscopy. A shorter wavelength produces more Raman scattering since Raman scattering intensity varies as the fourth power of frequency. For sample preparation the sample is grinded into fine powder. Solid sample is directly placed on the silicon wafer with for examine the sample. A glass substrate may also be used to characterize but features (properties) of glass may interfere the result.

4.3 Scanning electron microscopy

In Scanning electron microscopy (SEM) create a high resolution image of the sample by scanning the surface. It uses energy beam of electron to scan the sample surface. The electrons of electron beam interacts with atoms of sample surface there by producing different type electrons such as Backscattered electron and Secondary electron [4].

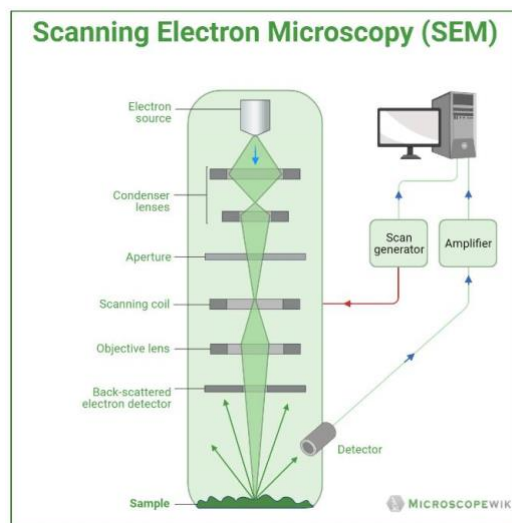


Figure 6: Schematic diagram of Scanning Electron Microscope [8].

Principle

Scanning electron microscopy works on the principle of scanning a sample with electron beams. The high accelerating electron beam is created by an electron gun which is passed down the column of the scanning electron microscope. The beam of electron pass through a series of lenses and apertures, which is used focus the beam of electrons. This process happens in vacuum conditions, which prevents the electron beam from interacting with molecules or atom in the chamber. It prevents the electron source from vibrations and noise. The electron beams scan the sample in a raster pattern with the help of scanning coil. The electrons interact with atoms on the surface of the sample and creates signals in the form of secondary electrons, backscattered electrons and rays that are characteristic of the sample. Detectors pick up these signals and create high-resolution images which is then displayed on a computer screen.

The components of SEM are Electron source, Anode ,Condenser lens, Scanning coils, Objective lens, Detectors to collect signals, Sample Stage, Display/Data output devices. Different types of electron guns used are such as TE (Thermionic- Emission) gun, FE (Field- Emission) gun, SE (Schottky- Emission) gun.

Sample stage

For non conductive sample a conductive coating is needed which is done with the help of sputter-coater. Conductive coats that can be used for coating are gold, silver, platinum and chromium.

Thermionic gun: in this tungsten filament is used as cathode or lanthanum hexaboride (LaB6) crystal. The cathode is heated to a very high temperature (around 2700 K for tungsten) by applying current which emits electrons at very high speed. Field emission gun: in this when a strong electric field is applied the potential barrier becomes low and thin, and the electrons are emitted by the tunneling effect. Schottky emission gun: Works on Schottky emission effect when high electric field is applied to heated metal surface.

The condenser lens controls the size of the beam and focus the electron beam on to the sample. The scanning coils are used deflect the beam along x and y direction. The objective lens is used to focus the beam to a very small spot on the sample. In SEM lenses are electromagnetic lens are used which are made up of a coil of wires inside metal poles and when a current passes through coils it will generate a magnetic field which helps in controlling electron beam.

To create vacuum turbomolecular and diffusion pump are used. So in order to create high vacuum low vacuum pump such as roughing pump is used first.

Everhart-Thornley (E-T) is used to detect secondary electrons. The Secondary electron are passed into the scintillator where they can be converted to light photons. The photon are passed to a photomultiplier tube for amplification. Backscatter electron detector is used to detect backscattered electron. Energy Dispersive X-ray Spectrometer Detector is used to detect characteristics X ray from the sample.

4.4 Photoluminescence (PL) spectroscopy

Photoluminescence it is defined as the process in which a molecule absorbs a photon and excites electrons to a higher electronic excited state, and which result in emission of excess energy in the form of luminescence which is called as photoluminescence. It may include the emission of light that is a radiative process or a non radiative process which does not emit light. Radiative transitions is due to absorption of a photon, if the transition take place to a higher energy level, or the emission of a photon, if the transition to a lower level. Non radiative transitions arises between Energy level of atoms or ions when there is no emission of Light.

Fluorescence and phosphorescence are the two forms of photoluminescence. Fluorescence, h has a short lifetime (10^{-8} to 10^{-4} s). Phosphorescence has the lifetime of usually from 10^{-4} – 10^{-2} s, much longer than that of Fluorescence. In fluorescence, high energy (short wavelength, high frequency) light is absorbed which excites an electron into an excited energy state. Generally the absorbed light is in ultraviolet range. Fluorescence happens so quickly that if you turn off the light the material stops glowing. A phosphorescent is a process which absorbs high energy light (usually ultraviolet) which excites the electrons to move into a higher energy state but make transition to a lower energy state occurs much more slowly. Phosphorescent materials glow for several seconds up to a couple of days even though the light has been turned off because the electrons jump to a higher energy level than for fluorescence as a result the electrons has to lose more energy and may spend time at different energy levels between the excited state and the ground state [5].

The setup generally consist a laser source, optical lenses, a placeholder for the sample to be placed and PL spectrometer. Only 1 cuvette is used which is filled with sample dispersed in solvent. Then the laser source is incident toward the optical mirror which directs the beam to the sample. When the laser beam is incident on to the sample, some electrons excites to higher energy levels and emits radiation when coming back to ground state which is then detected by the PL spectrometer at specific wavelengths. In this technique fixed wavelength is used to excite electrons and different wavelengths of light will be emitted. The light intensity is plotted against the wavelength on the spectrum.

The Absorbance spectrum can be created by exciting electrons at different wavelengths and monitoring the emission at a fixed wavelength. The resulting absorbance spectrum is important in determining the fixed excitation wavelength for the emission spectrum. So in this way emission spectrum cab be created by exciting electrons at a fixed wavelength and observing emissions at different wavelengths.

4.5 X-ray diffraction (XRD)

X-ray diffractometers consist of X-ray tube, sample holder, and X-ray Detector. X-rays are generated by heating a filament in a cathode ray tube so that accelerating electrons are produced which toward the target by applying a voltage resulting in bombarding the target material with electrons. When electrons have sufficient energy to knockout inner shell electrons of the target material and characteristic X-ray are produced. Filtering it by foils or crystal

Monochrometers will result in monochromatic X-rays. Commonly copper is used as target material with $\text{CuK}\alpha$ radiation = 1.5418\AA . X-rays are then collimated and are directed towards sample. Sample and detector are rotated and the intensity of the reflected X-rays is recorded. Constructive interference occurs when incident X-rays satisfies the Bragg Equation and a peak in intensity occurs. For constructive interference to occur the path difference should be integral multiple of the wavelength, λ . A detector records signal and then converts the signal to a count rate. X-ray detector is rotated at an angle of 2θ [6].

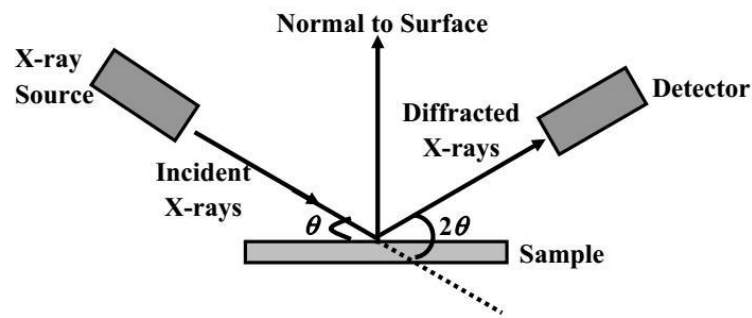


Figure 7: Schematic diagram of X-Ray Diffraction [9].

First grind the sample to a fine powder by mortar and pestle and then place into a sample holder. Then spreading it uniformly onto a glass slide which contain small cavity for sample to form flat upper surface .

References

- [1] Förster H. UV/vis spectroscopy. Characterization I: -/-. 2004 Feb 11:337-426.
- [2] Akash MS, Rehman K, Akash MS, Rehman K. Ultraviolet-visible (UV-VIS) spectroscopy. Essentials of pharmaceutical analysis. 2020:29-56.
- [3] Das RS, Agrawal YK. Raman spectroscopy: Recent advancements, techniques and applications. Vibrational spectroscopy. 2011 Nov 1;57(2):163-76.
- [4] Abd Mutalib M, Rahman MA, Othman MH, Ismail AF, Jaafar J. Scanning electron microscopy (SEM) and energy-dispersive X-ray (EDX) spectroscopy. In Membrane characterization 2017 Jan 1 (pp. 161-179). Elsevier.
- [5] Li Q, Anpo M, You J, Yan T, Wang X. Photoluminescence (PL) Spectroscopy. In Springer Handbook of Advanced Catalyst Characterization 2023 May 18 (pp. 295-321). Cham: Springer International Publishing.
- [5] Shih K. X-ray diffraction: Structure, principles and applications. Nova Science Publishers, Inc.; 2013.
- [6] <https://www.agilent.com/en/support/molecular-spectroscopy/uv-vis-upy/uv-vis-spectroscopy-spectrophotometer-basics>.
- [7] <https://www.edinst.com/blog/what-is-raman-spectroscopy/>
- [8] https://ciasalesk.live/product_details/7126427.html

[9]https://www.researchgate.net/figure/Schematic-Representation-on-the-Working-Principles-of-X-ray-Diffraction-30_fig5_334537641

CHAPTER 5: RESULT AND DISCUSSION

5.1 XRD analysis

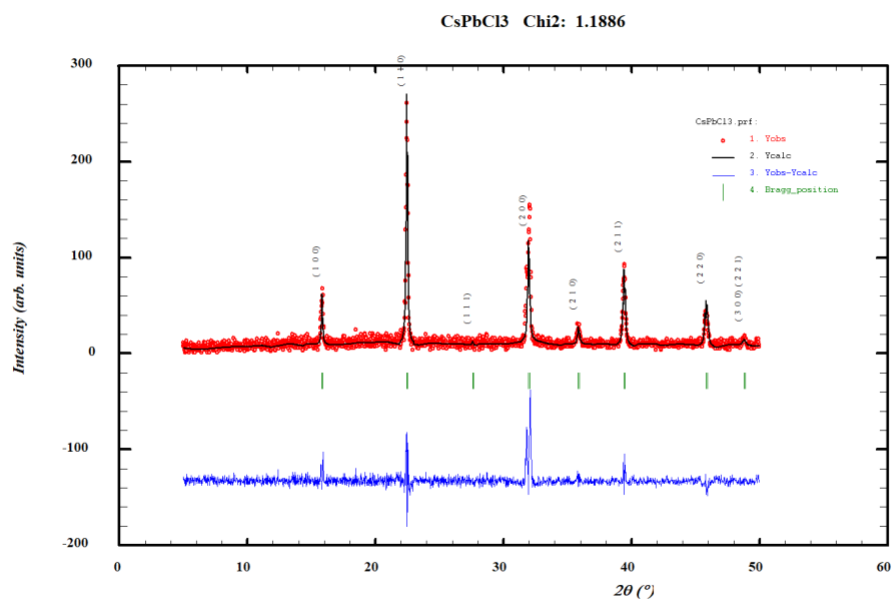
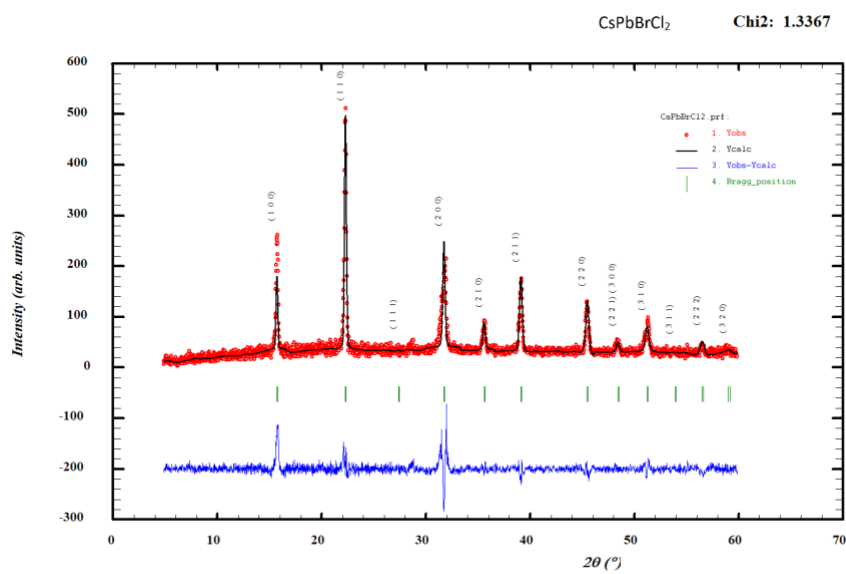
The structural properties of perovskites nanocrystals were studied using an X-ray powder diffraction (XRD) analysis, conducted on Rigaku Smart Lab Diffractometer using Cu-K α radiation ($\lambda = 1.5418 \text{ \AA}$). The figure below reports the experimental XRD pattern and the rietveld analysis of the prepared samples. The lattice parameter calculated for the samples were found to be $a=5.5976 \text{ \AA}$ for CsPbCl₃, $a= 5.63950 \text{ \AA}$ for CsPbCl₂Br₁, $a=5.6649 \text{ \AA}$ for CsPbCl_{1.5}Br_{1.5}, $a=5.6781 \text{ \AA}$ for CsPbCl₁Br₂, and $a=5.8363 \text{ \AA}$ for CsPbBr₃ which shows increase in the lattice parameter from chlorine to bromine [1]. It was also noticed that as the bromine concentration increases the (110) peaks shift to lower 2 theta angle indicating increase in lattice constant. By using the Scherrer equation that is

$$\frac{0.9 \lambda}{\beta \cos\theta}$$

and to calculate strain introduced in powder due to crystal imperfection and distortion is given as

$$\tau = \frac{\beta}{4 \tan\theta}$$

we found crystallite size and strain as 44.4nm and 0.2291 respectively for CsPbCl₃, 20.9 nm and 0.3454 for CsPbCl₂Br₁, 36.48 nm and 0.2826 A^o for CsPbCl_{1.5}Br_{1.5}, 47.44 nm and 0.2181 for CsPbCl₁Br₂, and 18.86 and 0.4184 for CsPbBr₃.

Figure 8: XRD spectra of CsPbCl₃Figure 9: XRD of CsPbCl₂Br₁

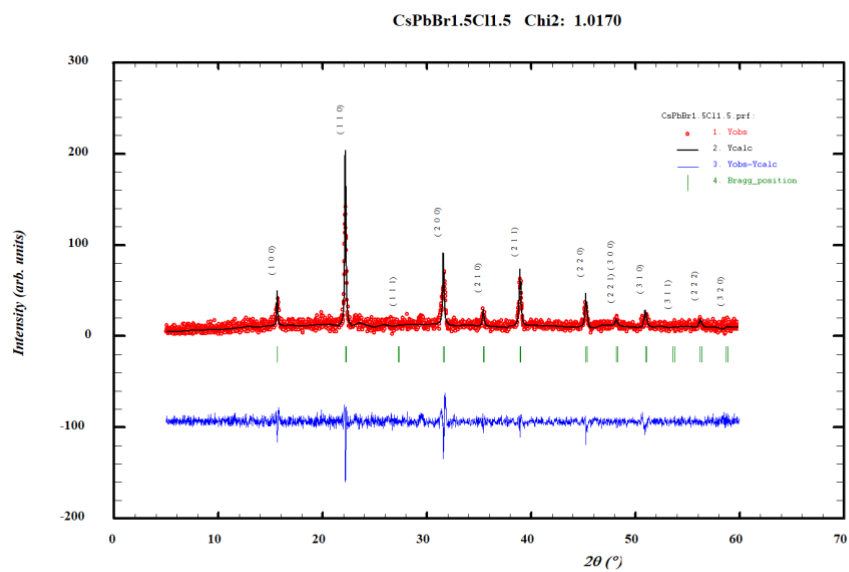


Figure 10: XRD of CsPbCl_{1.5}Br_{1.5}

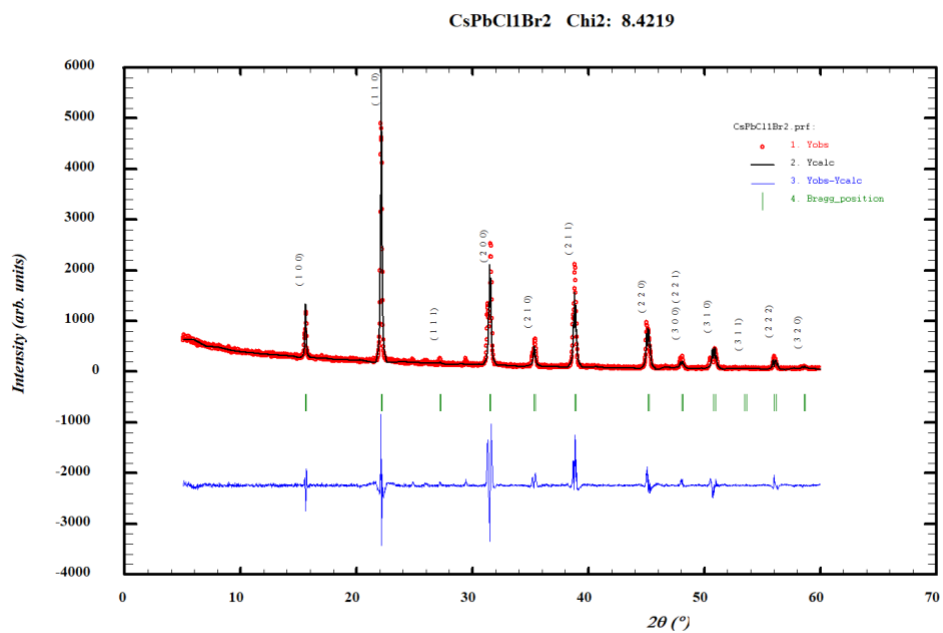


Figure 11: XRD of CsPbCl₁Br₂

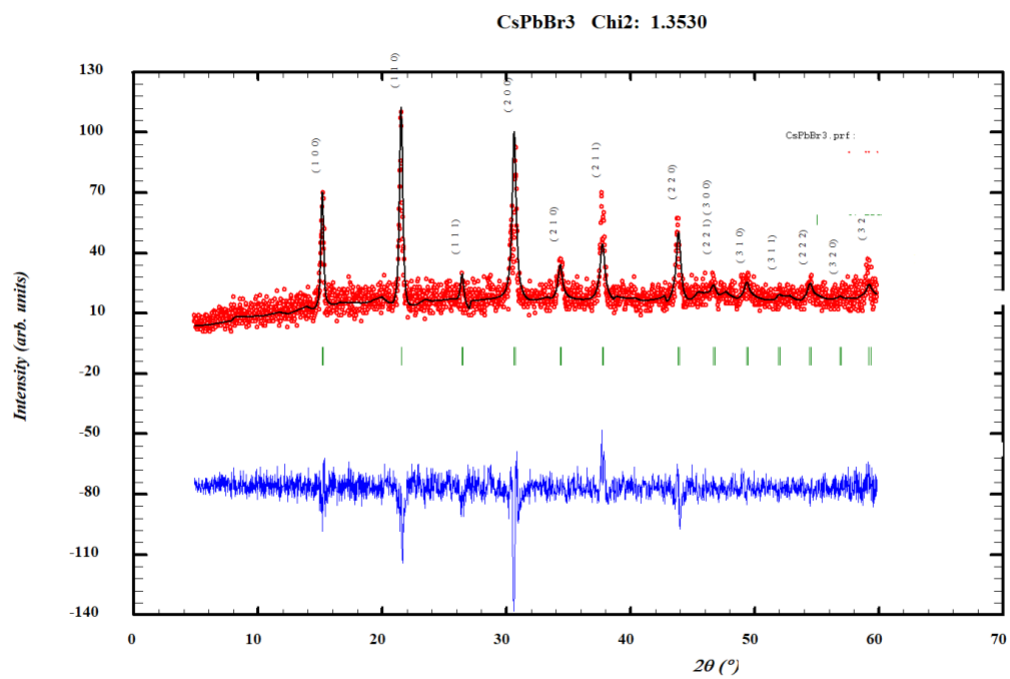


Figure 12: XRD of CsPbBr₃

5.2 UV Vis Spectroscopy analysis

UV-Vis spectra analysis was done using UV-Vis spectrometer. For finding the bandgap of synthesized material we used Tauc's plot.

The equation is given as:

$$(\alpha h\nu)^\gamma = A(h\nu - E_g)$$

Where, α is the absorption coefficient.

h is the Planck's constant.

ν is the photon's frequency.

A is a proportionality constant.

E_g is the band gap energy.

Γ denotes the nature of electronic transition.

Where $\gamma = 2$ for direct allowed transitions, $\gamma = 1/2$ for indirect allowed transitions.

$\Gamma = 2/3$ for direct forbidden transitions, $\gamma = 1/3$ for indirect forbidden transitions.

UV- Vis spectroscopic measurement was done for all prepared sample with powder UV-Vis spectroscopy setup. Figure 12 shows the absorption spectra of all samples. The absorption spectra showed increased in the absorption wavelength from CsPbCl_3 to CsPbBr_3 and their mixture of halide. For CsPbCl_3 the absorption was shown at 393 nm, for $\text{CsPbCl}_2\text{Br}_1$ absorption shown at 410 nm, for $\text{CsPbCl}_{1.5}\text{Br}_{1.5}$ absorption shown at 419 nm, for $\text{CsPbCl}_1\text{Br}_2$ absorption was shown at 429 nm and for CsPbBr_3 absorption was shown at 501 nm. It was seen that there is red shift in wavelength from Cl to Br.

From the Tauc's plot shown in the figure (7,8,9,10,11) below shows decrease in the bandgap from CsPbCl_3 to CsPbBr_3 and their mixture of halide. . For CsPbCl_3 the bandgap was found to be 2.88 eV, for $\text{CsPbCl}_2\text{Br}_1$ the bandgap was 2.75 eV, for $\text{CsPbCl}_{1.5}\text{Br}_{1.5}$ the bandgap was 2.66 eV, for $\text{CsPbCl}_1\text{Br}_2$ the bandgap was 2.63 eV, CsPbBr_3 the bandgap was 2.24 eV. The bandgap of CsPbCl_3 is the highest (2.88 eV) and CsPbBr_3 has the lowest (2.24 eV). With increasing concentration of Br in $\text{CsPbCl}_1\text{Br}_{1-x}$ the bandgap was found to decrease. Increase in the ionic radii from Cl to Br which results in increase of bond length. Smaller bond length results in tight binding of electrons inside the atom therefore more energy is required to remove the electrons which leads to increase in the bandgap. [2]

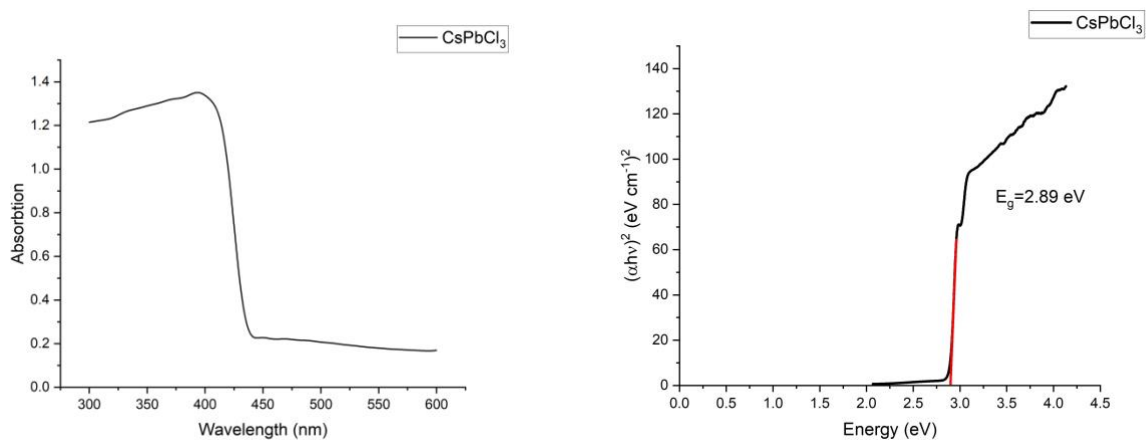


Figure 13: Absorption and Bandgap of CsPbCl₃

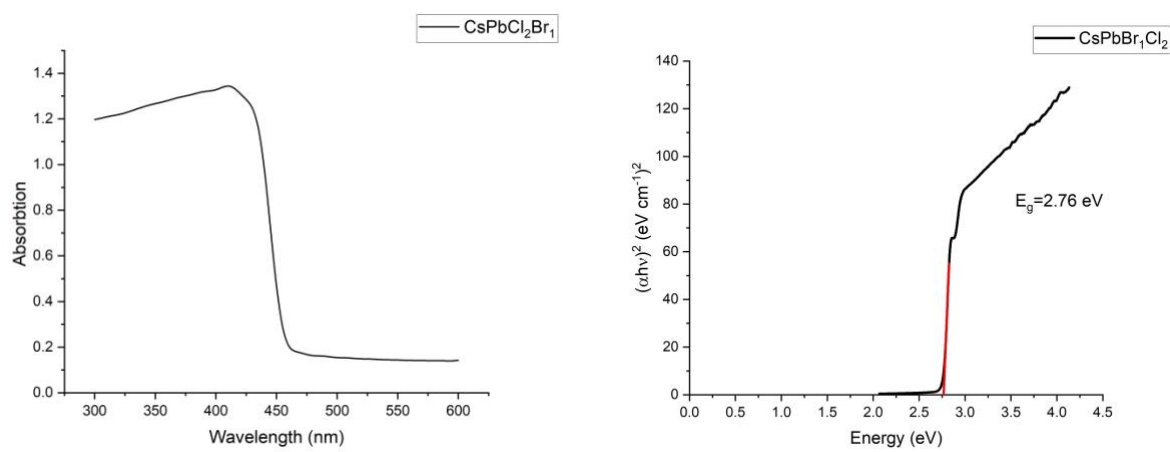


Figure 14: Absorption and Bandgap of CsPbCl₂Br₁

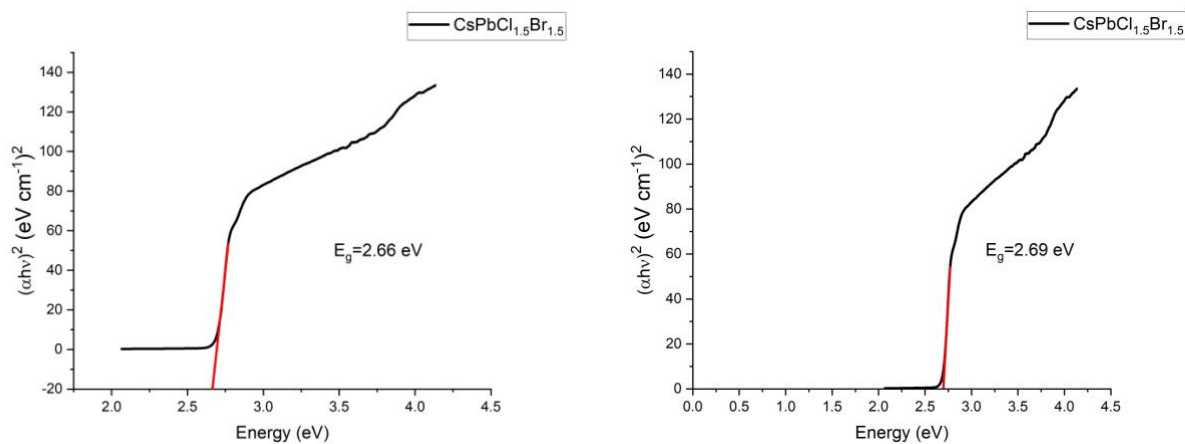


Figure 15: Absorption and Bandgap of $\text{CsPbCl}_{1.5}\text{Br}_{1.5}$

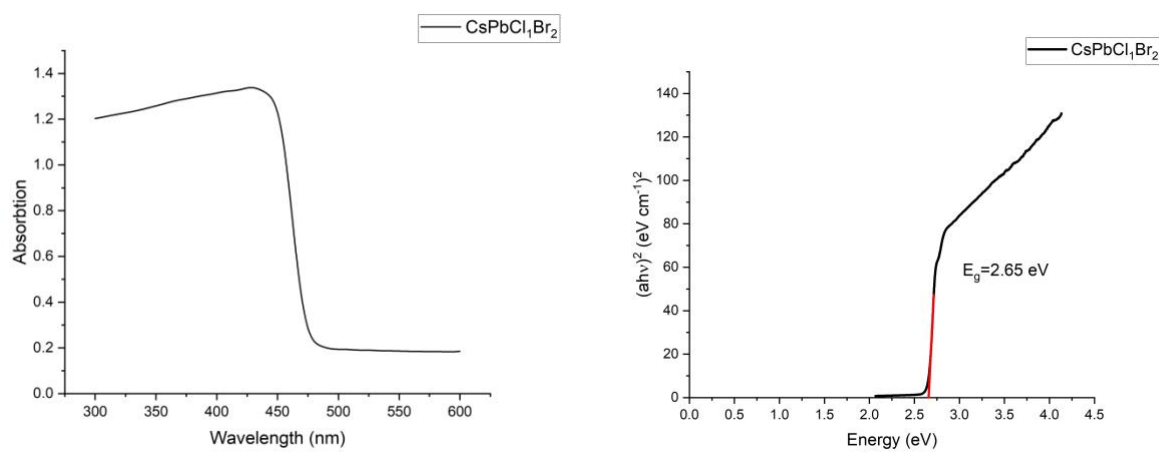


Figure 16: Absorption and bandgap of $\text{CsPbCl}_1\text{Br}_2$

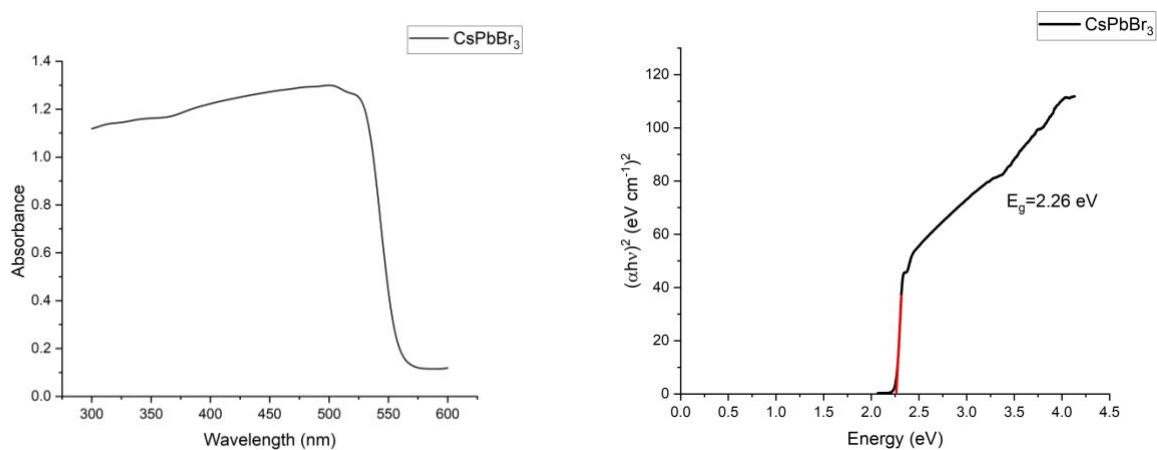


Figure 17: Absorption and bandgap of CsPbBr₃

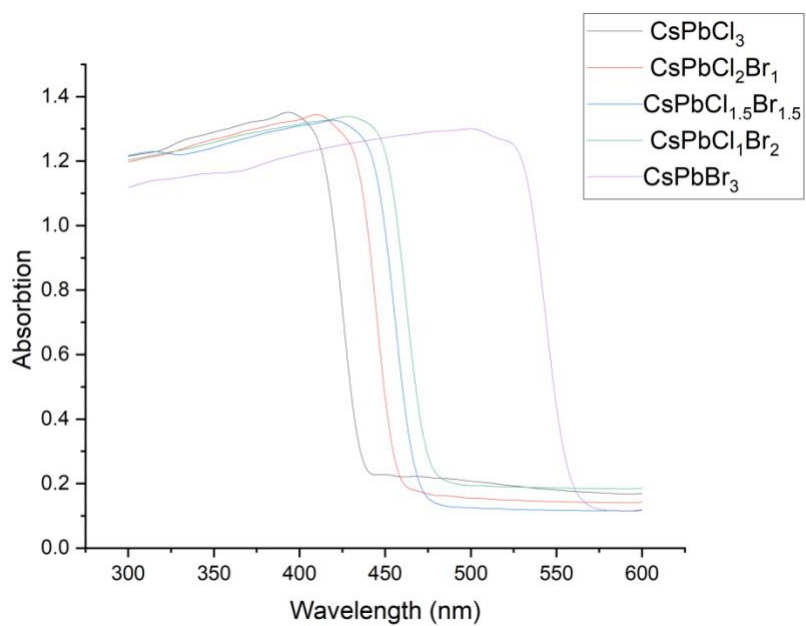


Figure 18: Figure showing absorption of all samples

5.3 Photoluminescence spectroscopy analysis

We have also investigated the room temperature photoluminescence spectra of all samples. All the samples were excited at 360 nm light source. The PL emission of CsPbCl_3 and CsPbBr_3 and their mixed halide composition are shown in the figure 16 below. PL emission spectra of halide perovskites are strongly depended on the halide composition which can be seen from the figure below. The Photoluminescence spectra showed increased in the emission wavelength from CsPbCl_3 to CsPbBr_3 and their mixture of halide. For CsPbCl_3 the emission peak was shown at 428 nm, for $\text{CsPbCl}_2\text{Br}_1$ emission peak shown at 421 nm, for $\text{CsPbCl}_{1.5}\text{Br}_{1.5}$ emission peak shown at 463 nm, for $\text{CsPbCl}_1\text{Br}_2$ emission peak was shown at 474 nm and for CsPbBr_3 emission peak was shown at 530 nm. It was seen that there is red shift in wavelength from Cl to Br. So the prepared samples exhibits optical tunability from 428 nm to 530 nm by simply change the halide composition.

With increase in the atomic number of halide element from chlorine to bromine, the bond strength decreases between Pb and X. As a result the valence and the conduction band move closer to each other and reduces the optical bandgap. The observed red shift in the PL emission wavelength peak in CsPbX_3 with increase concentration of bromine which results in bandgap quenching phenomenon.[3]

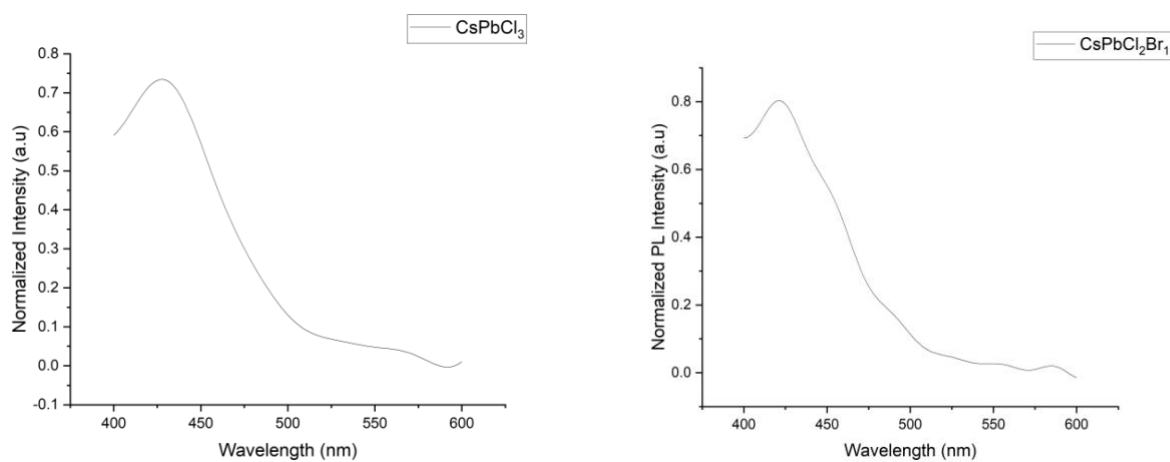


Figure 19: PL spectra of CsPbCl_3 and $\text{CsPbCl}_2\text{Br}_1$

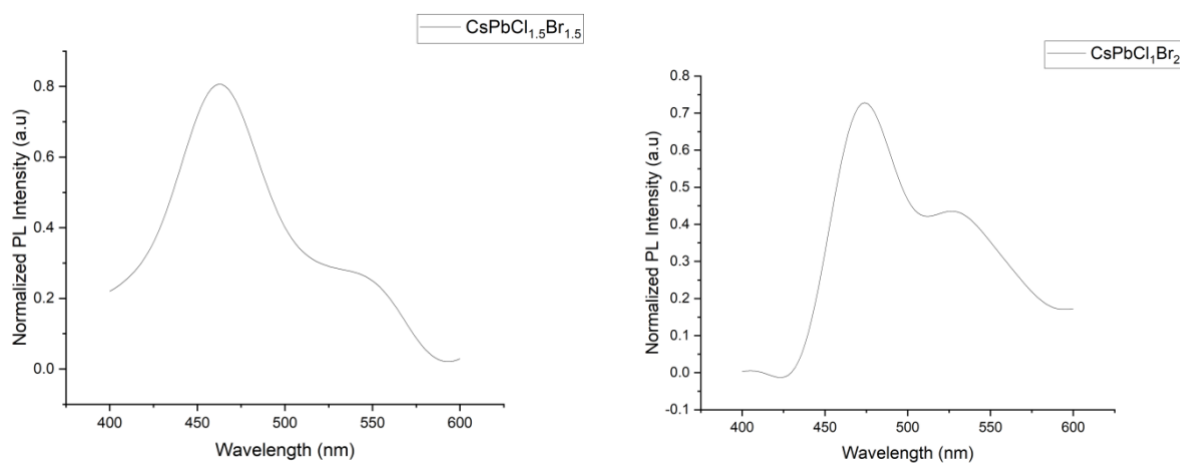


Figure 20: PL spectra of $\text{CsPbCl}_{1.5}\text{Br}_{1.5}$ and $\text{CsPbCl}_1\text{Br}_2$

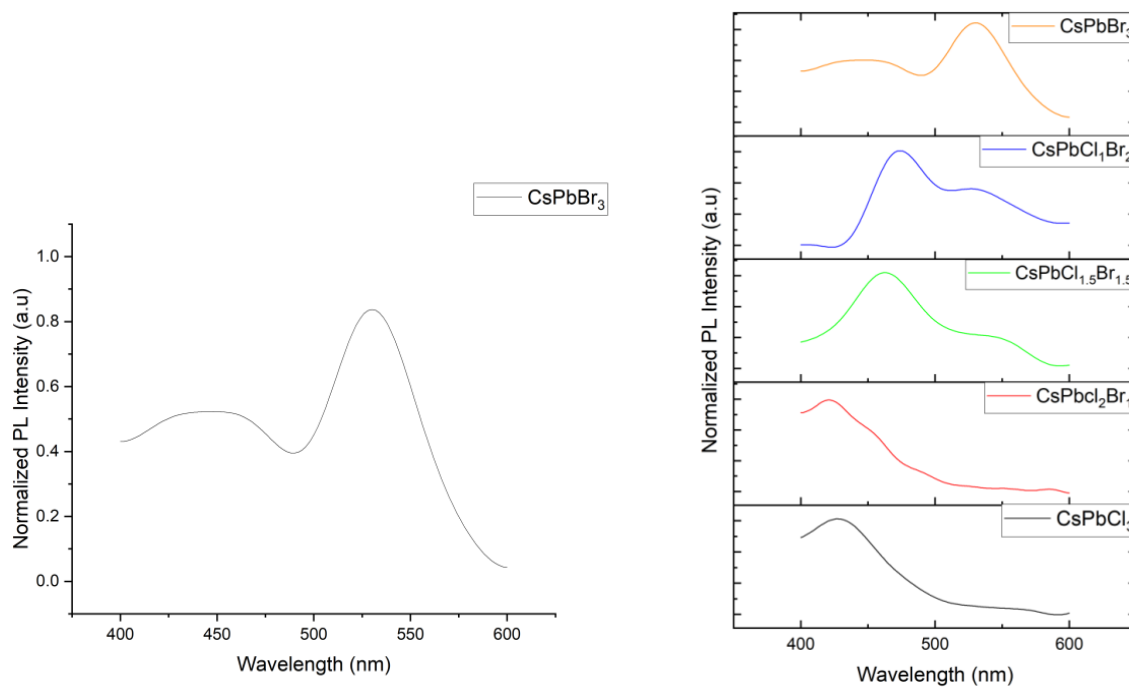


Figure 21: PL spectra of CsPbBr_3 and PL spectra of all samples

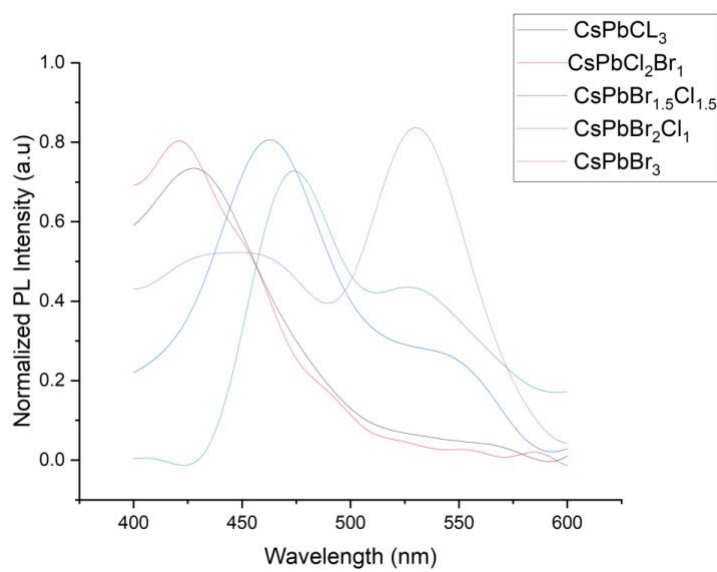


Figure 22: PL spectra of all samples

5.4 Scanning Electron Microscope Analysis

The morphology of the as prepared samples was studied using the Carl Zeiss Scanning Electron Microscope (SEM). The SEM images were analyzed using the ImageJ software of the as prepared samples was determined.

The cubic structure of all prepared synthesis can be seen in the below figure with good morphology and crystalline size.[4]

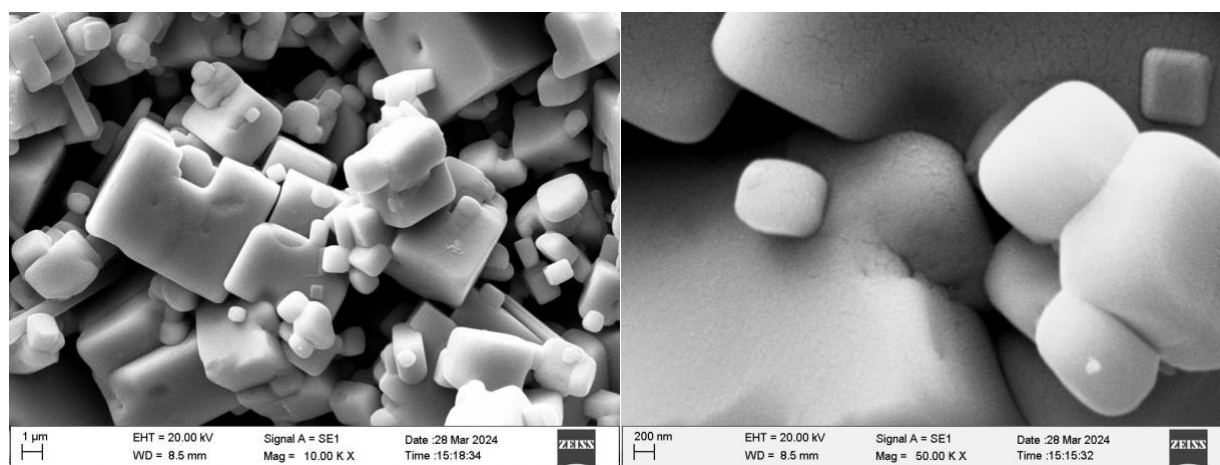


Figure 23: SEM images of CsPbCl₃

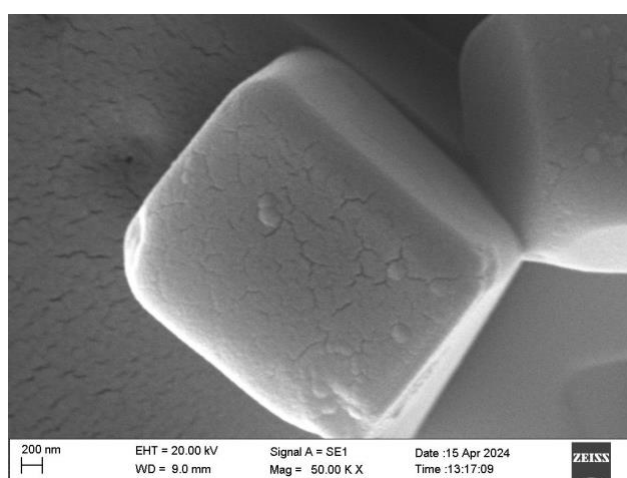
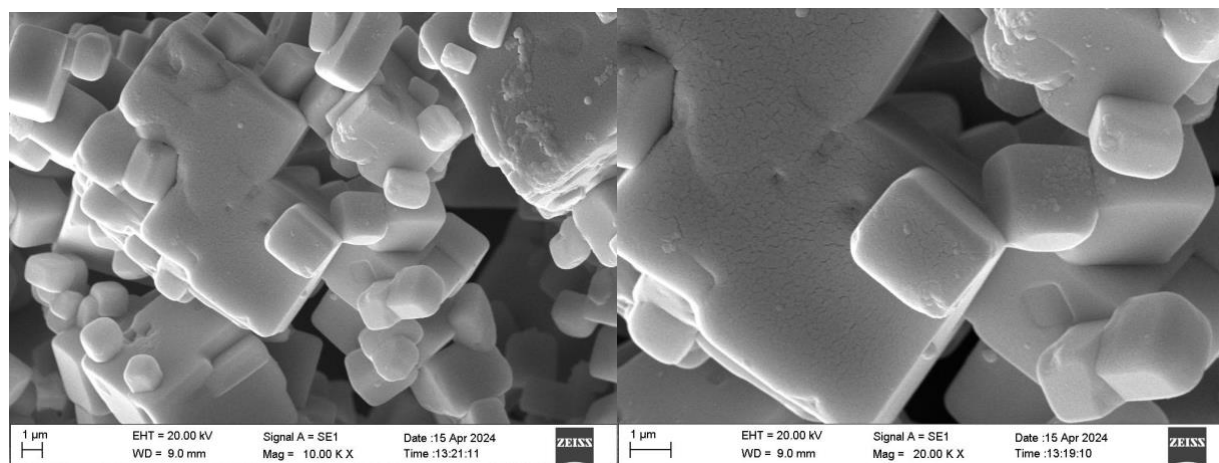


Figure 24: SEM images of CsPbCl₂Br₁

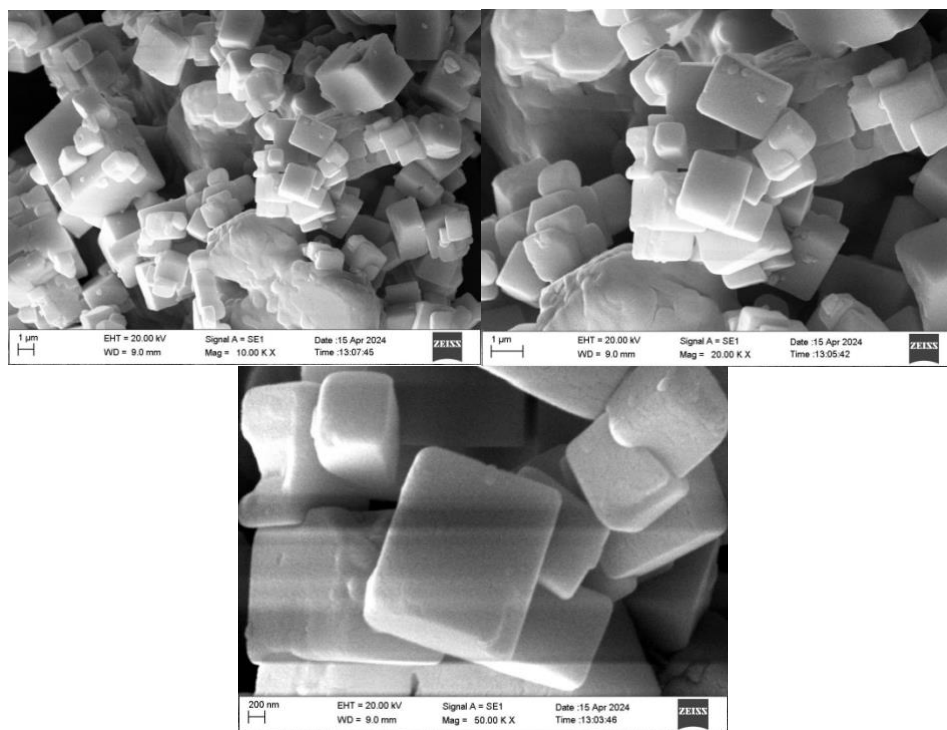


Figure 25: SEM images of CsPbCl_{1.5}Br_{1.5}

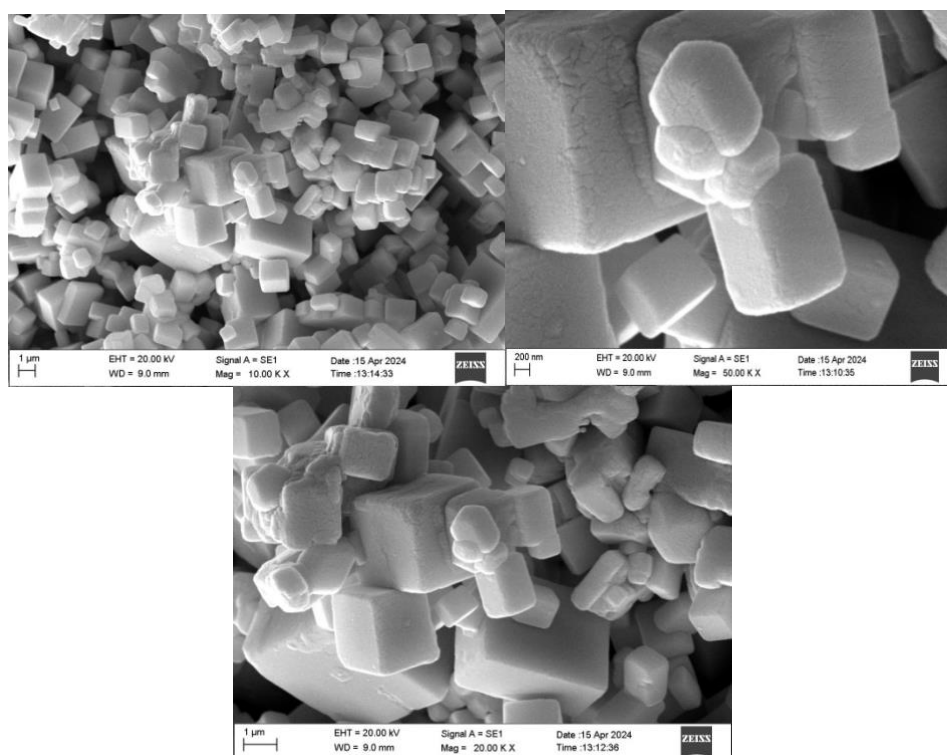


Figure 26: SEM images of CsPbCl₁Br₂

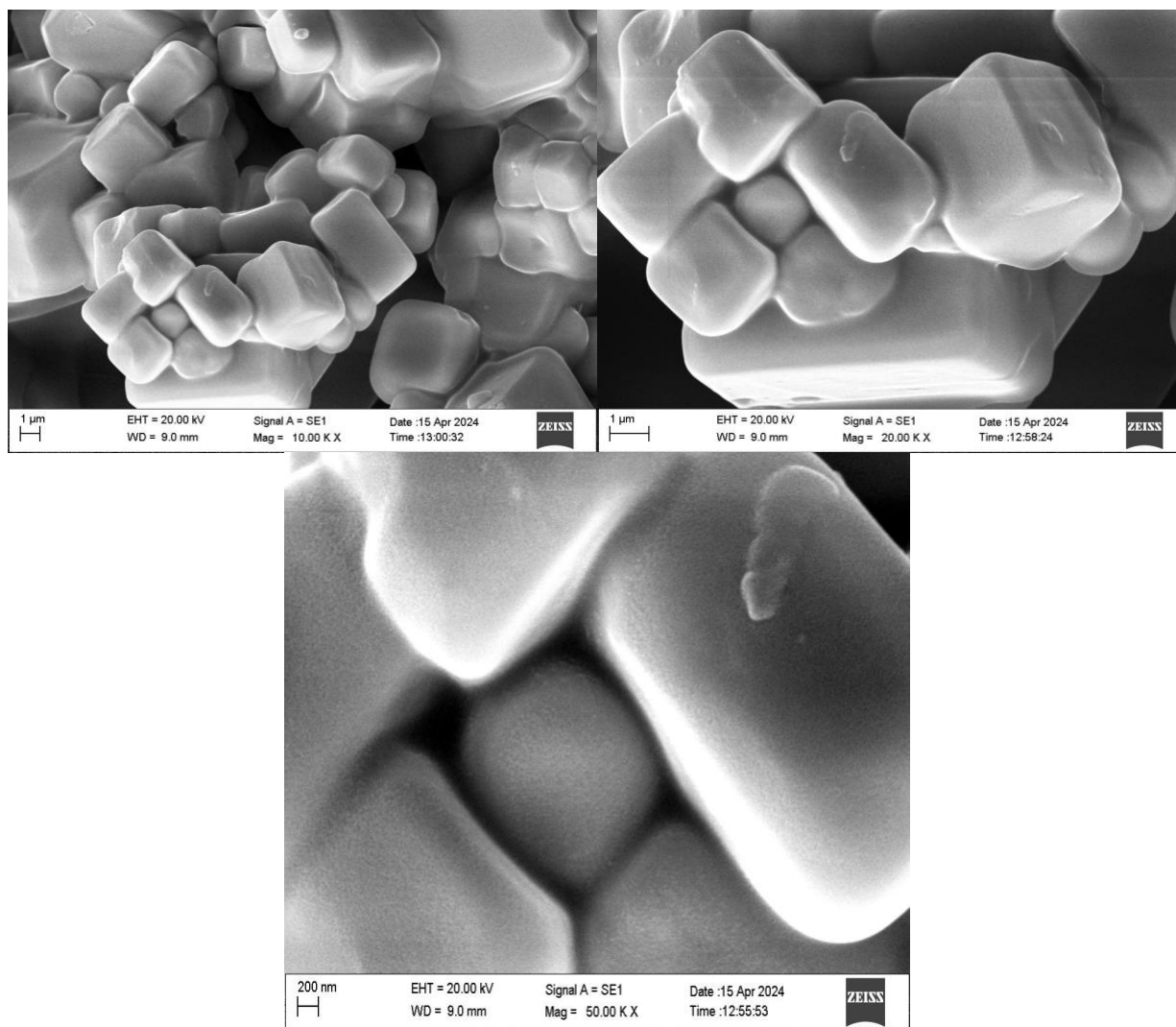


Figure 27: SEM images of CsPbBr₃

5.5 Raman spectroscopy analysis

In the raman spectra we can see active modes at $(68,86)\text{cm}^{-1}$, $(94,121)\text{cm}^{-1}$, and $(173,220)\text{cm}^{-1}$.

The $(94,121)\text{cm}^{-1}$ correspond to $[\text{PX}_6]$ octahedron while the $(173,220)\text{cm}^{-1}$ correspond to motion of cesium. Its was seen that upon increasing the bromide concentration there is a blue shift in raman. So as we go from bromine to chloride the bond length between Pb-X decreases which result in the increase of vibrational frequency and leading to crystal structure contraction.

For CsPbBr_3 we get two raman peaks at 106cm^{-1} and 228cm^{-1} . [5]

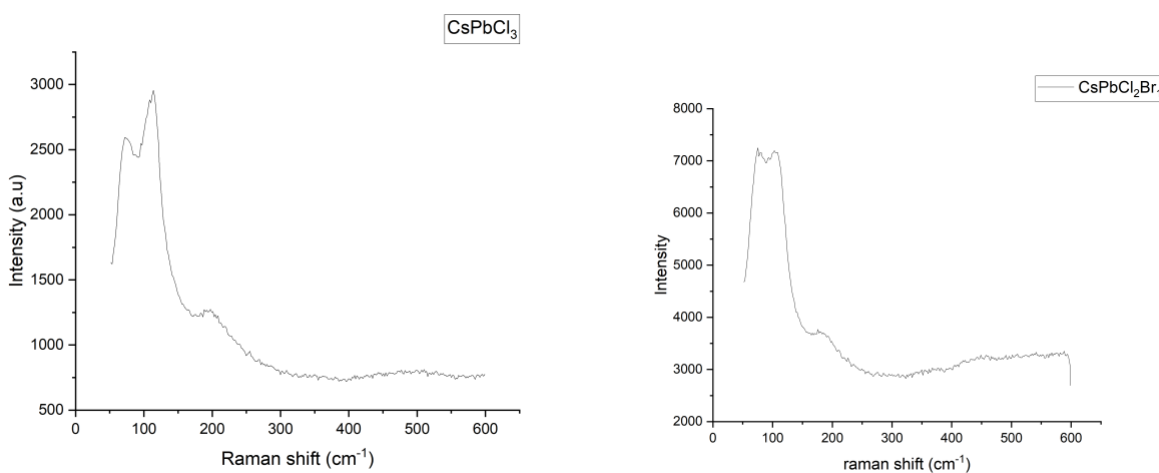


Figure 28: Raman spectra of CsPbCl_3 and $\text{CsPbCl}_2\text{Br}_1$

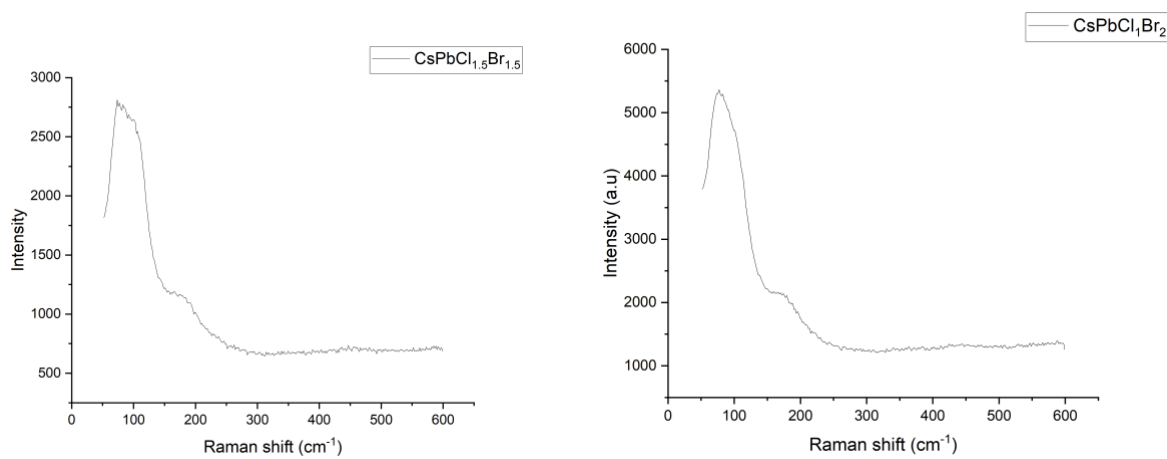


Figure 29: Raman spectra $\text{CsPbCl}_{1.5}\text{Br}_{1.5}$ and $\text{CsPbCl}_1\text{Br}_2$

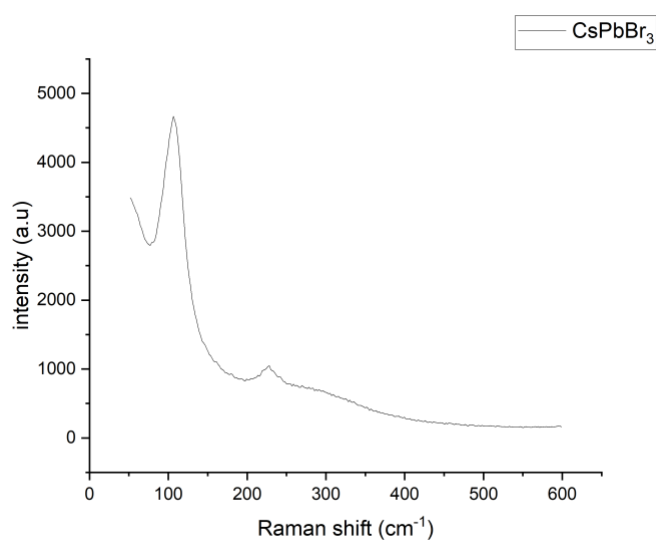


Figure 30: Raman spectra of CsPbBr_3

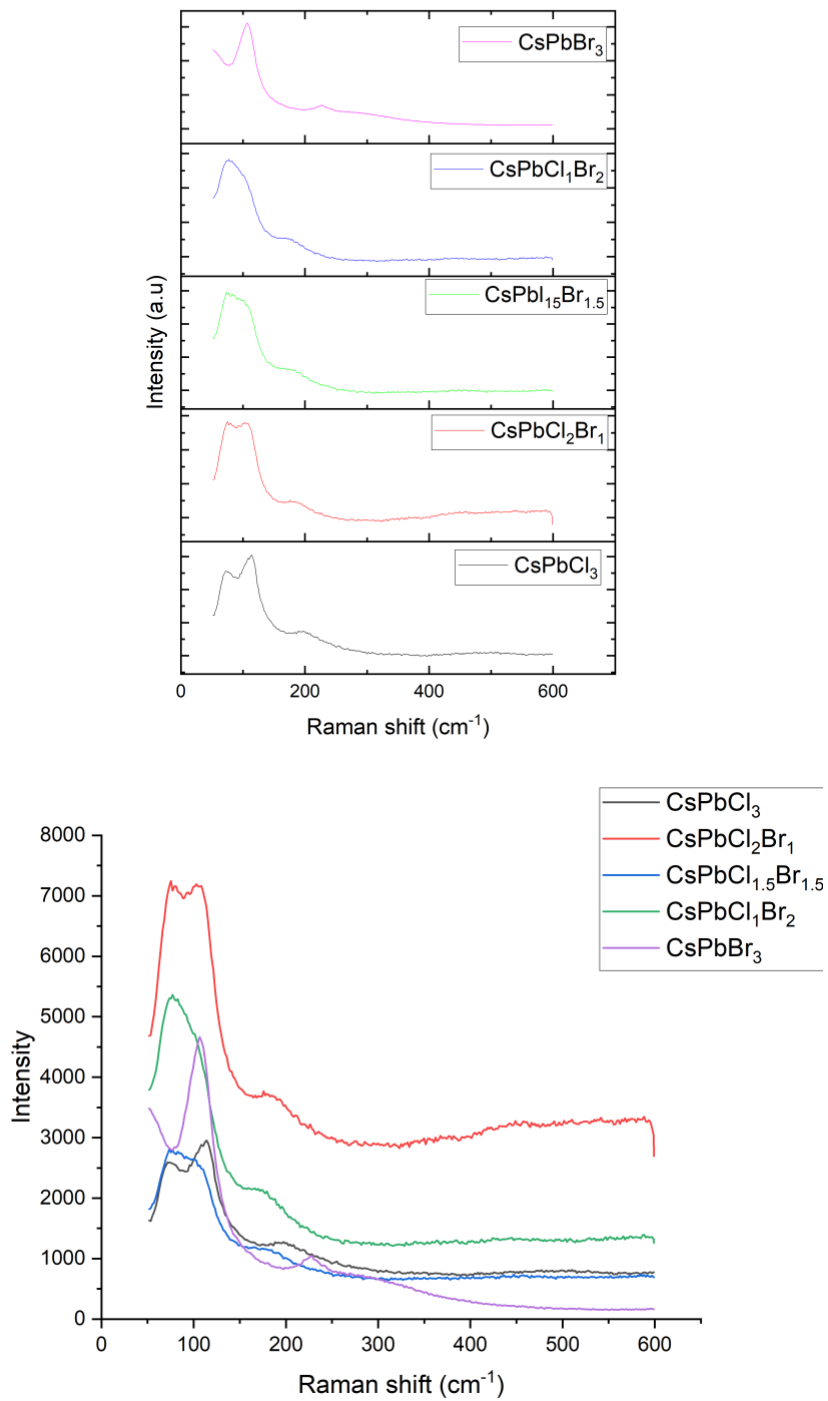


Figure 31: Raman spectra of all samples

References

- [1] Chen M, Zou Y, Wu L, Pan Q, Yang D, Hu H, Tan Y, Zhong Q, Xu Y, Liu H, Sun B. Solvothermal synthesis of high-quality all-inorganic cesium lead halide perovskite nanocrystals: from nanocube to ultrathin nanowire. *Advanced Functional Materials*. 2017 Jun;27(23):1701121.
- [2] Roy M, Vikram, Banerjee S, Mitra A, Alam A, Aslam M. Composition-Controlled Synthesis of Hybrid Perovskite Nanoparticles by Ionic Metathesis: Bandgap Engineering Studies from Experiments and Theoretical Calculations. *Chemistry—A European Journal*. 2019 Jul 25;25(42):9892-901.
- [3] Gai C, He D, Wang Y, Wang J, Li J. Engineering of Halide Cation in All-Inorganic Perovskite with Full-Color Luminescence. *Coatings*. 2021 Mar 13;11(3):33.
- [4] Yang D, Chu S, Wang Y, Siu CK, Pan S, Yu SF. Frequency upconverted amplified spontaneous emission and lasing from inorganic perovskite under simultaneous six-photon absorption. *Optics Letters*. 2018 May 1;43(9):2066-9.
- [5] Thesika K, Vadivel Murugan A. Microwave-enhanced chemistry at solid–liquid interfaces: synthesis of all-inorganic CsPbX₃ nanocrystals and unveiling the anion-induced evolution of structural and optical properties. *Inorganic chemistry*. 2020 Apr 14;59(9):6161-75.

CHAPTER 6: CONCLUSION

Ligand assisted reprecipitation method has been successfully used to synthesize $\text{CsPbCl}_{3-x}\text{Br}_x$ ($x=0,1,1.5,2,3$) perovskites structure at room temperature. This method requires precise control over temperature during the synthesis process. All samples crystallized into cubic structure having pm3m phase group. Also the lattice parameter was found to increase from 5.5976 Å to 5.8363 Å by increasing the bromine content in $\text{CsPbCl}_{3-x}\text{Br}_x$ which resulted in decrease of (110) peak to lower angle. Crystalline size was found to vary from 44 nm to 18 nm for all prepared samples. Absorption wavelength was seen to increase from 393 nm to 501 nm and bandgap was found to decrease from 2.89 eV to 2.26 eV. Photoluminescence spectra showed red shift in the emission wavelength with increasing bromine content in $\text{CsPbCl}_{3-x}\text{Br}_x$. From SEM spectroscopy revealed a cubic morphology for all samples. The Raman spectroscopy showed three active modes for CsPbCl_3 and two active modes for CsPbBr_3 . The raman shift decreases as we increase the bromine concentration since there was increase in the bond length between Pb-Br which resulted in decrease of the vibrational frequency.